SAN DIEGO STATE UNIVERSITY AND

UNIVERSITY OF CALIFORNIA

Santa Barbara

The Tale of Western Chitwan Community Forests: Historical Vegetation Dynamics and the Challenges with the Invasion of *Mikania micrantha*

A Dissertation submitted in partial satisfaction of the

requirements for the degree Doctor of Philosophy

in Geography

by

Jie Dai

Committee in charge:

Professor Li An, Chair

Professor Dar A. Roberts

Professor Douglas A. Stow

Professor Phaedon C. Kyriakidis

September 2020

The dissertation of Jie Dai is approved.

_____

Phaedon C. Kyriakidis

_____

Dar A. Roberts

_____

Douglas A. Stow

_____

Li An, Committee Chair

September 2020

The Tale of Western Chitwan Community Forests: Historical Vegetation Dynamics and the Challenges with the Invasion of *Mikania micrantha*

ACKNOWLEDGEMENTS

This research was funded by the National Science Foundation under the Dynamics of Coupled Natural and Human Systems program (grant BCS-1211498) and the National Aeronautics and Space Administration Earth and Space Science Fellowship (grant 80NSSC17K0317), and also by the Inamori Fellowship, William & Vivian Finch Fellowship, and Analytical Spectral Devices (ASD) Goetz Student Support Program. I thank San Diego State University, University of California, Santa Barbara and the Geography Department at both institutions for research support. I am grateful to my committee Drs. Li An, Dar Roberts, Doug Stow and Phaedon Kyriakidis for inspiring and supporting my research. I acknowledge input and support from Drs. Scott Yabiku, Sharon Hall, Dirgha Ghimire, Qunshan Zhao and Michele Clark. I also acknowledge the support of the staff at the Institute for Social and Environmental Research – Nepal, in particular Krishna Shrestha, Indra Chaudhary, and Krishna Ghimire, and thank them for hosting me during my fieldwork in Nepal. To my parents, I am forever grateful for your support and understanding. Thank you.

VITA OF JIE DAI

September 2020

EDUCATION

Doctor of Philosophy in Geography, San Diego State University and University of California, Santa Barbara, September 2020 (expected)

Master of Science in Natural Resources and Environment, University of Michigan, Ann Arbor, 2013

Bachelor of Engineering in Spatial Informatics, Wuhan University, China, 2011

PROFESSIONAL EMPLOYMENT

Fall 2013 – Spring 2018: Teaching Associate, Department of Geography, San Diego State University

Winter 2013: Graduate Student Instructor, School of Natural Resources and Environment, University of Michigan, Ann Arbor

PUBLICATIONS

Dai, J., D. Roberts, D. Stow, L. An, S. Hall, S. Yabiku & P. Kyriakidis (2020). Mapping understory invasive plant species with field and remotely sensed data in Chitwan, Nepal. *Remote Sensing of Environment* 250, 112037.

Dai, J., D. Roberts, P. Dennison & D. Stow (2018). Spectral-radiometric differentiation of non-photosynthetic vegetation and soil within Landsat and Sentinel 2 wavebands. *Remote Sensing Letters* 9(8), 733-742.

Dai, J. & L. An (2018). Time Geography. In Huang, B. (Ed.), *Comprehensive Geographic Information Systems*, Vol. 1, pp. 303-312. Oxford: Elsevier.

An, L. & J. Dai (2017). Space-time Analysis. In Lin, H., X. Shi, X. Ye, and Y. Guan (Ed.), *Frontiers in Geographic Information Science* (in Chinese). Beijing: Advanced Education Press.

Zhao, Q., E. Wentz, S. Fotheringham, S. Yabiku, S. Hall, J. Glick, J. Dai, M. Clark & H. Heavenrich (2016). Semi-parametric geographically weighted regression (S-GWR): A case study on invasive plant species distribution in subtropical Nepal. *The 9th International Conference on Geographic Information Science*, 396-399.

PRESENTATIONS AND POSTERS

Understory Mikania micrantha Mapping with Field and Remotely Sensed Data in Chitwan, Nepal (AGU Fall Conference, San Francisco, CA, 2019)

Urbanization, Protected National Park, and Community Forestry: Land Cover Change in Chitwan, Nepal, 1988-2018 (AAG Annual Meeting, Washington D.C., 2019)

Spectral-radiometric differentiation of non-photosynthetic vegetation and soil within Landsat and Sentinel 2 wavebands (ASPRS Annual Meeting, Denver, CO, 2018)

Linking Forest Health with Vulnerability to an Invasive Plant Species: A Case Study in Chitwan, Nepal (AAG Annual Meeting, Tampa, FL, 2014)

AWARDS

NASA Earth and Space Science Fellowship (2017-2020)

Third Place, AAG Remote Sensing Specialty Group Student Paper Competition (2020)

ASPRS Pacific Southwest Region Scholarship (2019)

William & Vivian Finch Scholarship in Remote Sensing (2018-2019)

Graduate Student Travel Fund, San Diego State University (2018 & 2019)

ASD Goetz Instrument Student Support Program, Malvern Panalytical (2018)

Inamori Fellowship (2017-2018)

Geography Department Citizenship Award, San Diego State University (2017)

ABSTRACT

The Tale of Western Chitwan Community Forests: Historical Vegetation Dynamics and the Challenges with the Invasion of *Mikania micrantha*

by

Jie Dai

This dissertation addresses the historical vegetation dynamics in community forests, their novel challenges introduced by the invasion of an exotic creeping vine, and simulations of large-scale intervention practices in western Chitwan, Nepal. Situated in the Chitwan National Park buffer zone, these community forests stand as the frontiers of human-environment interactions, nurturing both endangered large mammals such as Bengal tigers (*Panthera tigris tigris*) and great one-horned rhinos (*Rhinoceros unicornis*), as well as local forest users. For the past three decades, especially after their establishments in the mid-1990s, these forests have been greening up. In addition to community forest management, some of the green-up signals may be affected by the invasion of a notorious understory creeping vine, *Mikania micrantha*. Integrating remote sensing techniques (Multiple Endmember Spectral Mixture Analysis) and species distribution modeling (Maximum Entropy Modeling Framework), we developed a pixel-based presence probability map for the invasive plant in the study area. By the year 2015, the invasion was most prominent in riverine forests and riparian grasslands. To combat the

spread of *M. micrantha* in the study area, we tested a cost-effective bag-and-bury treatment and developed a socio-ecological data informed agent-based model to project local household participation in an intervention program as well as *M. micrantha*'s extent under the intervention practices. Both social survey and simulation results indicated that about 40% of the households in the study area can contribute at least ten full days of labor per year to the modified intervention treatments, and *M. micrantha* can be eliminated from the community forests after three years of intensive intervention, although routine patrolling should be adopted to eradicate potential future invasion from the neighboring national park. This dissertation incorporated a coupled human and natural systems (CHANS) approach and integrated both social and ecological factors. The results can provide significant insights for not only local conservation practices, but also broader sustainable managements and development goals.

Table of Contents

List of Tables

List of Figures

1. Chapter I: Introduction

Understanding the dynamics of ecosystems, their services, and human impacts on their trajectories is one of the fundamental goals concerning sustainability, and the rapidly changing world requires effective ecological assessment and forecasting for future management (Craig 2010; Dietze et al., 2018 Milly et al., 2008). Since the mid-1950s, global population has been increasing at an alarming rate, causing large-scale deforestation and natural resource exploitation (Ezeh et al., 2012). To mitigate the pressure of population growth on deforestation and forest degradation while sustaining human wellbeing, community forests have been established worldwide, especially in developing countries (Gilmour 2016). These forests incorporate autonomous management from local residents in varying degrees, aiming to preserve forest ecosystem services while sustainably maintaining local residents' livelihoods (Gilmour 2016).

Funded by the National Science Foundation, a multi-disciplinary research team has been examining the "feedbacks between human community dynamics and socioecological vulnerability" (National Science Foundation grant BCS-1211498) in the western Chitwan community forests, Nepal. Based on this coupled natural-human (CNH) project, this dissertation addresses the historical vegetation dynamics, the novel challenges introduced by the invasion of an understory creeping plant, and simulations of large-scale intervention practices in these community forests. The study site includes an internationally recognized national park and biodiversity hotspot, as well as its buffer zone community forests and their catchment area households. Examining the current level of invasion and understanding possible scenarios of future forest conditions are critical to sustainable community forest management.

The research integrates a social survey with regression analysis and computer simulations to study vegetation dynamics and effects of invasive species intervention on forest conditions.

The Chitwan district is located in the central part of Nepal bordering India to the south. It is famous for the Chitwan National Park, recognized as a World Heritage site and a significant biodiversity hotspot in the Terai region of Nepal with elevation between 120 and 815 m, nurturing endangered great one-horned rhinoceros (*Rhinoceros unicornis*), Bengal tiger (*Panthera tigris tigris*) and other endemic species (UNESCO 2020; CEPF 2020). Chitwan is also home to about 600,000 people who live and farm nearby (Central Bureau of Statistics-Nepal, 2011). Beginning in the 1950s, large-scale deforestation occurred as forest was converted to farmland. To mitigate the pressure of deforestation as well as sustaining the livelihoods of local residents, the Nepali government implemented the Community Forestry Act in 1993 (Nagendra 2002; Spiteri & Nepal, 2008). Since the mid-1990s, 21 community forests have been established in the national park buffer zone. These community forests are characterized by incorporating local residents in forest management, and in Chitwan, residents form autonomous committees to regulate forest use and provide financial supports for the forest members (Charnley & Poe, 2007).

Not long after their establishments, these community forests were encountered with considerable challenges of biological invasion. Since the late 1990s, an understory creeping vine, *Mikania micrantha*, has been invading the national park and its buffer zone community forests (Murphy et al., 2013). *M. micrantha* is nicknamed “mile-a-minute vine” due to its ferocious speed of growth and it is one of the world’s most notorious invaders (IUCN 2020). It decreases forest productivity by hindering the growth of native species, weakens social

organizations that manage and shape households' resource use in the community forests, and downgrades local ecosystems and their corresponding services (Murphy et al. 2013). The invasion of *M. micrantha* is jeopardizing the western Chitwan community forests and has the potential of totally disrupting local coupled human and natural systems.

The body of this dissertation is comprised of three chapters (Chapters II-IV) and a synthesis and concluding section (Chapter V). Chapter II examines the vegetation dynamics in the western Chitwan community forests from 1988 to 2018. In particular, it evaluates how green vegetation fractions has been changed. Chapter III models and develops a pixel-based *M. micrantha* distribution map in the community forests and the national park. Chapter IV draws on field experiments and computer simulations to predict how *M. micrantha* invasion in the forests will respond to planned intervention practices. Finally, Chapter V reviews the primary findings of the preceding chapters and identify potential future research directions.

2. Chapter II: Community Forests Continuously Green-up since Their Establishments in Western Chitwan, Nepal

2.1 Introduction

Community forestry, characterized by incorporating local communities and individuals into forest management, aims at preserving forest ecosystem services while sustainably maintaining local residents' livelihood, especially in Global South countries (Gilmour 2016). It has a wide spectrum of organizational structures, ranging from private smallholder forestry to government-designated preservation lands with limited local involvement (Gilmour 2016; RECOFTC 2013). Community forests have been extended globally in the past four decades and cover about 732 million hectares of land, or 18.2% of the world's forest area, playing significant roles in mitigating many serious environmental and social problems, including climate change and poverty alleviation (Gilmour 2016).

Monitoring forest cover is critical in community forest management, and remote sensing techniques have been applied in assessing vegetation conditions and dynamics (Coppin & Bauer, 1996; Kim et al., 2014; Potapov et al., 2008). One concise and effective method is to calculate and examine vegetation indices, including the most widely used index, the Normalized Difference Vegetation Index (NDVI), where higher values are associated with greater vegetation cover and stature (Huete 1988; Liu & Huete 1995; Qi et al., 1994; Rouse et al., 1973). Despite being simple, these indices may sometimes produce controversial results due to undesirable atmospheric conditions or mixture effects from background substrate (Huete et al., 1985; Saleska et al., 2005; Samanta et al., 2010; Shen et al., 2013; Zhang et al., 2013). An alternative approach is to apply spectral mixture analysis to the selected imagery and

analyze the resultant vegetation fractions and indices developed from these fractions (Adams et al., 1995; Roberts et al., 1998; Souza Jr. et al., 2005; Souza Jr. et al., 2013). By incorporating both reference and image spectra in the endmember sets and quantifying the constituent fractions of major land cover types (e.g. Green Vegetation, Non-Photosynthetic Vegetation, and Soil, etc.), spectral mixture analysis can address mixed pixels, minimize atmospheric effects, and bypass inconsistences of wavelengths in different sensor types, which are common issues in long-term research utilizing moderate spatial resolution multispectral imagery (Roberts et al., 1998; Souza Jr. et al., 2005; Souza Jr. et al., 2013).

The western Chitwan community forests in Nepal was established in the Chitwan National Park buffer zone following the Community Forestry Act implemented in 1993 (Nagendra 2002). These community forests serve as frontiers of human-environment interactions between protect area and rural residential landscapes. They are vital to both the survival of endangered mammals and the livelihoods of local residents (Murphy et al., 2013). However, few studies have systematically examined the vegetation cover changes in these forests since their establishment. This chapter evaluates vegetation cover dynamics in the western Chitwan community forests for the past three decades utilizing a temporal series of Landsat imagery. Particularly, it addresses the changes before and after the implementation of Community Forestry Act in 1993, and the potential effects of forest managements on the vegetation cover dynamics. Since the rivers flow sinuously through most of the riverine forests, this chapter first examined their water fraction dynamics. It then applied spectral mixture analysis to selected Landsat imagery and analyzed the green vegetation fractions of green vegetation (GV), non-photosynthetic vegetation and soil. The Normalized Difference Fractional Index (NDFI; Souza

Jr. et al., 2005) was also calculated to evaluate forest canopy gaps. Both GV fractions and NFDI were adjusted to minimize the effects of water bodies at the forest level. The results will demonstrate the vegetation dynamics in the past three decades and provide important feedbacks to community forest committees and users.

2.2 Methodology

2.2.1 Study Area

The Chitwan District situates in the central region of Nepal, bordering India to the south. It is known mostly for the Chitwan National Park, which is a World Heritage Site designated by the United Nations Educational, Scientific and Cultural Organization (UNESCO 2020). It is also a significant biodiversity hotspot, nurturing Bengal Tiger (*Panthera tigris tigris*), Great One-horned Rhino (*Rhinoceros unicornis*) and other endemic species (CEPF 2020). Since the 1950s, deforestation and urbanization have converted much of local forests in Chitwan to agricultural and other land-cover types. To protect the remaining natural resources, mitigate anthropogenic pressures on conservation, and sustain local residents' livelihoods, community forests were established following the Community Forestry Act in 1993 (Nagendra 2002; Spiteri & Nepal, 2008). These forests are buffer zones between dense human settlements and the protected national park, and users are granted limited access to the forests to extract livelihood resources such as firewood and fodder. This chapter focuses on 21 community forests in the Chitwan National Park buffer zone (Fig. 2-1).

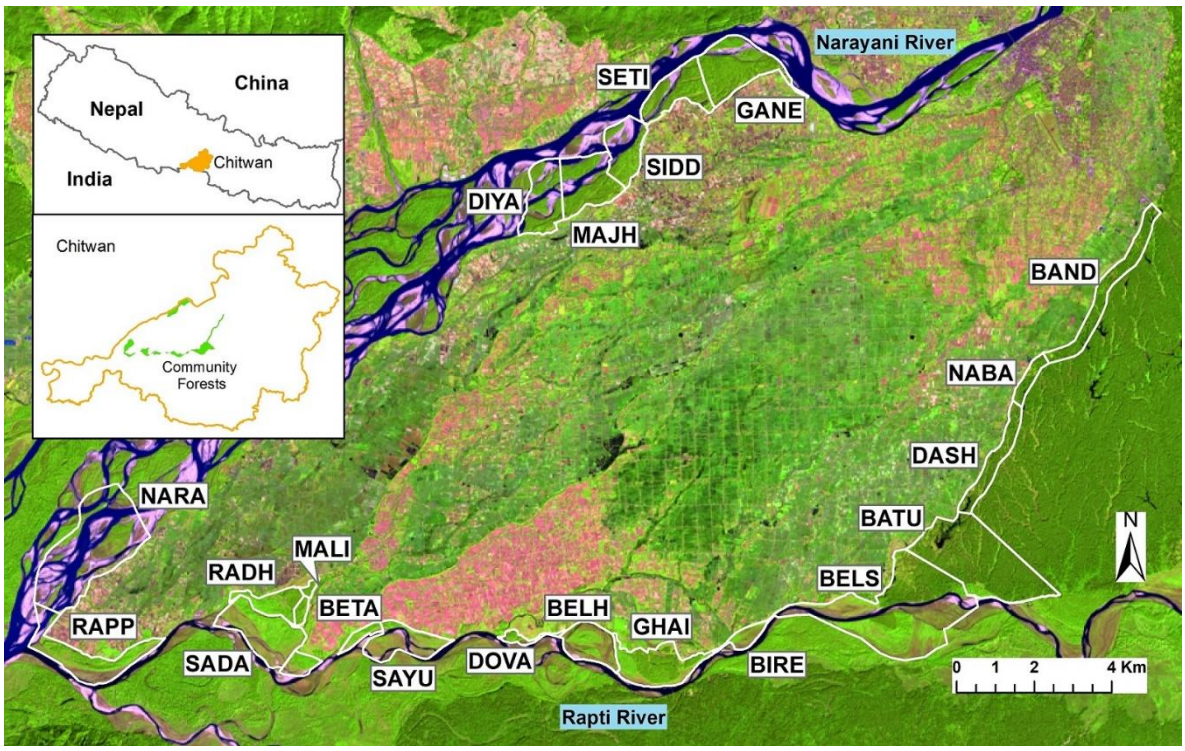

Figure 2-1: False color Landsat 8 three-band composite of the study area. White polygons depict the community forest boundaries, with forest codes illustrated. Image acquisition date: Oct. 27, 2014. Red: Band 6 (1560-1660 nm); Green: Band 5 (845-885 nm); Blue: Band 4 (630-680 nm).

Most of the forests were established along the Narayani and Rapti Rivers, where riverine mixed forests are the dominant vegetation types, supplemented by riparian grasslands. The most common plant species in these riverine forests include *Acacia catechu*, *Bombax cieba*, *Dalbergia sissoo*, *Maesa chisia*, *Melia azedarach* and *Trewia nudiflor*. The four inland forests (BAND, NABA, DASH and BATU), however, are dominant by Sal trees (*Shorea robusta*). The study area has a tropical monsoon climate with mean annual precipitation of 2100 mm and most of the rain falling from June through early October. Average daily temperature ranges from 36 °C in the summer to 18 °C in January. For the purpose of this chapter, the 21 forests were categorized into five groups (Table 2-1).

Table 2-1: Community forests in the study area

Group	Forest Name	Code	Area (km^2)
East Sal	Bandevi	BAND	1.62
	Nabajoty	NABA	0.42
	Dashinkali	DASH	1.05
	Batuliphokhari	BATU	4.57
South Central Rapti	Belshar	BELS	6.40
	Birendranagar	BIRE	0.40
	Ghailaghari	GHAI	1.82
	Belhatta	BELH	1.21
	Dovan	DOVA	0.23
South West Rapti	Sayukta Rapti Doon	SAYU	1.36
	Betarihariyali	BETA	0.87
	Malika	MALI	0.11
	Radhakrishna	RADH	0.82
	Sadabahar	SADA	2.10
Far West	Rapptiniyantran	RAPP	2.06
	Narayani Niyantran	NARA	5.01
North Narayani	Diyalo	DIYA	1.66
	Majhuwa	MAJH	1.86
	Siddhi Ganesh	SIDD	1.35
	Seti Debi	SETI	1.51
	Ganeswor	GANE	2.27

2.2.2 Data

Due to the timespan of the research objective (dating back into the 1980s), this chapter incorporated Landsat imagery (Path/Row: 142/41) in USGS EarthExplorer (https://earthexplorer.usgs.gov/) and potential Landsat surface reflectance products (Level-2; TM, ETM+ and OLI) were investigated. Searching criteria included: 1) image acquisition dates are within a two-month window after the monsoon (roughly between late September and mid-November) to account for peak-biomass conditions and 2) images are cloud-free above the study area. If multiple images met the above two criteria, the earliest available was selected. Consequently, at least one image was identified for most of the years (Table 2-2).

Table 2-2: Landsat imagery and their calendar and Julian dates

Year	Date	Julian	Sensor	Year	Date	Julian	Sensor
1988	10/19	293	TM	2005	11/19	323	TM
1989	11/07	311	TM	2006	10/05	278	TM
1991	11/13	317	TM	2008	10/26	300	TM
1992	11/15	320	TM	2009	10/29	302	TM
1993	10/17	290	TM	2011	10/19	292	TM
1994	10/20	293	TM	2013	11/19	323	OLI
1995	11/08	312	TM	2014	10/27	300	OLI
1996	11/10	315	TM	2015	10/14	287	OLI
2000	09/26	270	ETM+	2016	11/01	306	OLI
2001	10/31	304	ETM+	2017	10/19	292	OLI
2003	11/14	318	TM	2018	10/22	295	OLI
2004	10/15	289	TM				

In addition to satellite imagery, during fieldwork in September 2018, *in situ* reference spectra were collected for major herbaceous species (including *M. micrantha*) at 1 m height with a nadir view geometry under cloud-free conditions within 2 hours of solar noon in the community forests, with sunlight as the light source. Spectra of other common land cover types were also collected in the study area, including soil, non-photosynthetic vegetation (NPV; e.g. senesced grass, plant residue, etc.; Roberts et al. 1993) and gravel fields (categorized as Soil here) in the study area. Spectroscopic surface reflectance data were collected with an Analytical Spectral Devices (ASD) FieldSpec® 4 Standard-Res spectroradiometer (Malvern Panalytical, Westborough, MA). Equipped with three detectors spanning the visible and near infrared (VNIR) and shortwave infrared (SWIR1 and SWIR2), the instrument samples at a spectral range of 350-2500 nm, with a sampling interval of 1.4 nm for the VNIR detector, and 1.1 nm for SWIR detectors. The Full Width Half Maximum is 3 nm in VNIR and 10 nm in the SWIR. With a 25-degree field of view, the 1.5 m fiber optic cable transmits light from the aperture to the spectrometer. Each plant spectrum was sampled 10 times to account for random errors and was bracketed by measurements from a Spectralon white reference panel to offset any changes

in solar illumination or changes due to weather. The reflectance values, automatically calibrated from the radiance records in the field, were later extracted through the software package ViewSpecPro (Malvern Panalytical, Westborough, MA).

2.2.3 Methods

One of the challenges in quantifying vegetation cover in the study area was the water body dynamics in the community forests. The Narayani and Rapti Rivers flow sinuously across most riverine forests (Fig. 2-1). Besides, annual monsoon and the consequent rainfall can submerge large portions of the riverine forests, especially the riparian grasslands, altering water body boundaries frequently. Since this chapter examines vegetation cover in the forests, information within the forest boundaries would be aggregated to the forest-level. To minimize potential influences of water on detected vegetation dynamics, the water coverage was first quantified in all forests, and water-adjusted green vegetation fractions and NDFI were calculated to analyze the change trends.

2.2.3.1 Water coverage

To quantify the water coverage in the forests, this chapter incorporated the Automatic Water Extraction Index (AWEInsh; Feyisa et al., 2014) to map surface water in the study area:

$$AWEI_{nsh} = 4(Green - SWIR1) - (0.25NIR + 2.75SWIR2), \quad (1)$$

where Green, SWIR (Short-Wave Infrared) 1, NIR (Near Infrared) and SWIR2 are the reflectance values of corresponding bands (Table 2-3). Based on visual interpretation, an $AWEI_{nsh}$ threshold of 0.1 was used to generate water masks and dichotomize the imagery into water and non-water regions, where pixels with $AWEI_{nsh}$ value higher than 0.1 are assigned to water. Next, zonal statistics (mean) was applied to calculate the average water fractions of each

community forest polygon, $Water_{zonal}$.

Table 2-3: Landsat bands used in $AWEI_{nsh}$

Bands	TM/ETM+	OLI
Green	Band 2 (520-600 nm)	Band 3 (525-600 nm)
NIR	Band 4 (760-900 nm)	Band 5 (845-885 nm)
SWIR1	Band 5 (1550-1750 nm)	Band 6 (1560-1660 nm)
SWIR2	Band 7 (2080-2350 nm)	Band 7 (2100-2300 nm)

2.2.3.2 Spectral Mixture Analysis

SMA is a classic method quantifying spectrally mixed pixels, especially for moderate and coarse spatial-resolution imagery. It assumes that an image pixel's spectral reflectance can be modeled as the weighted addition of the reflectance of pure materials, or endmembers, within that pixel (Adams et al., 1995; Roberts et al., 1998). Developed upon simple SMA, multiple endmember SMA (MESMA) allows the type and number of endmembers to vary on a per-pixel basis, accounting for potential endmember varieties (Roberts et al., 1998). In this chapter MESMA was applied to the selected Landsat imagery.

For most vegetated landscapes, the image pixels can usually be modeled as a Green Vegetation (GV), Non-photosynthetic Vegetation (NPV), Soil and Shade mixture. To apply MESMA, spectral libraries were developed across endmember types incorporating endmember variability for different sensor types (TM/ETM+ and OLI). Ground reference spectra, including Green Vegetation (GV), NPV and Soil, were acquired through *in situ* measurements. Complimentary NPV and Soil spectra were identified from two online spectral libraries: (1) Jet Propulsion Laboratory (JPL) ASTER Spectral library (Baldridge et al., 2009), and (2) USA Geological Survey (USGS) Spectral Library (Kokaly et al., 2017). All candidate reference spectra were convolved to Landsat 8 OLI wavelength in the software package ENVI (Harris Geospatial Solutions, Boulder, CO). Candidate image spectra, including GV, NPV and Soil,

were extracted by drawing representative region of interest (ROI) polygons in the Landsat imagery and including all pixels in the polygons. Image spectra identified through applying Pixel Purity Index (PPI) were also included.

Combining all candidate reference and image spectra, subsets of spectra were identified from the library through Endmember Optimization module in Viper Tools, an ENVI add-on module (Roberts et al., 2007). For each bright endmember type (GV, NPV and Soil), the spectra with the lowest Endmember Average Root-mean-square-error (EAR; Dennison & Roberts, 2003), lowest Mean Average Spectral Angle (MASA; Dennison et al., 2004) and highest Count-Based Endmember Selection (COB; Roberts et al., 2003) score were selected. In the case of a tie with COB, EAR was used to split the tie. This subset was considered a reasonable balance between MESMA processing time and endmember variabilities.

The comprehensive endmember sets were used to unmix the selected Landsat imagery. Physically reasonable ranges were set to [0, 1] for bright endmembers (GV, NPV and Soil) fractions. The allowed range for Shade fractions was [0, 0.5]. The most complex endmember combinations were four-endmember models (4-EM; three bright EMs plus Shade). All combination sets (2-EM, 3-EM and 4-EM; Table 2.4) were tested for each pixel, and the one that generates the lowest root-mean-square-error (RMSE) was selected as the candidate model. If this RMSE was no higher than 0.025, the candidate model was selected, otherwise the pixel was left unmodeled.

Table 2-4: Allowed models by endmember types with total model numbers in parentheses

Two-endmember (7)	**Three-endmember (16)**	**Four-endmember (12)**
GV + Shade	GV+ NPV + Shade	GV + NPV + Soil + Shade
NPV + Shade	GV + Soil + Shade	
Soil + Shade	NPV + Soil + Shade	

To validate the fractions of bright endmembers (e.g. GV, NPV and Soil) in MESMA results, a 5-m spatial resolution RapidEye image captured on Nov 29, 2013 was obtained to generate reference data. Since the imagery type and MESMA procedures were consistent among the three years (2013-2015), the validation of one year's image would be sufficient. MESMA fractions were first shade-normalized before validation. 100 random points were generated in the study area, and the corresponding pixels were assigned as candidate validation pixels. After excluding points that fall out of the reference image or points where pixels were not modeled by MESMA (e.g. water, cloud, shadow, etc.), 67 pixels were left for validation. Through unsupervised classification in ERDAS and with the aid of Google Earth high spatial-resolution imagery, the reference image was classified into GV, NPV, Soil and other cover types, including water, cloud and shadow. For each bright endmember type (GV, NPV and Soil), using the centroid of the 67 validation pixels as the focal points, the focal statistics (sum) at a neighborhood setting of 6 by 6 cells (30 m by 30 m) were analyzed. In this way, the sum divided by 36 would be the reference fraction of that pixel. In the end, validation pixels were assessed using R^2 derived from plotting MESMA fractions (y) against reference fractions (x).

MESMA generated fractional layers for each bright endmember (GV, NPV and Soil) as well as Shade. At the pixel level, the green vegetation fractions were shade-normalized:

$$GV_{Shade} = GV / (1 - Shade), \quad (2)$$

where GV and Shade were the fractions generated in MESMA. Next, the average green vegetation fraction of each community forest, GV_{zonal}, was processed through zonal statistics (mean). To account for water area, the water-adjusted green vegetation fraction was calculated:

$$\text{Water-adjusted GV} = GV_{zonal} / (1 - Water_{zonal}), \quad (3)$$

where $Water_{zonal}$ was the forest-level average water fraction calculated in Section 2.2.3.1. It should be noted that shade normalization is a pixel-based adjustment, whereas water adjustment is an area-based correction over a region (each community forest).

2.2.3.3 Normalized Difference Fraction Index (NDFI)

NDFI ([16]) was also calculated to examine and sharpen the signals of canopy damage and gaps in the forests:

$$NDFI = (GV_{Shade} - (NPV + Soil)) / (GV_{Shade} + (NPV + Soil)), \quad (4)$$

where GV_{shade} was the shade normalized GV fraction calculated in Equation (2); NPV and Soil were the fractions generated in MESMA. In the end, forest-level average NDFI values, $NDFI_{zonal}$, were calculated through zonal statistics (mean) analyzes.

2.2.3.4 Forest dynamics

Although Landsat images were selected from roughly similar times of the year to account for peak-biomass vegetation conditions, the Julian dates of image acquisitions still differed considerably (Table 2-2), which could lead to fluctuations in vegetation dynamics. Instead of conducting a yearly-based time series analysis and because of some limited imagery availability, the 1988-2018 timespan was divided into four periods to analyze forest dynamics (Table 2-5). Period I accounts for forest conditions before the establishments of community forests in 1993, and Periods II, III and IV relate to post-establishment conditions. For each period, Landsat images from multiple years were selected so that the average Julian dates were similar among different periods. To identify potential significant changes between any two periods, forest-level average water-adjusted GV_{shade} and NDFI values (from Sections 2.2.3.2 and 2.2.3.3) of each period were compared through one-tailed two sample unequal variance T-

tests (e.g. Periods I vs. II, II vs. III, III vs. IV, I vs. III, II vs. IV and I vs. IV), where all values in the same period were treated as a sample. Comparisons between Period I and all later periods (I vs. II-IV) were also conducted to evaluate the potential effects of 1993 Community Forestry Act on forest dynamics.

Table 2-5: Selected Landsat imagery for different periods

Periods	Years Selected
I (Pre 1993)	1988, 1989, 1991, 1992, 1993
II (1994-1999)	1994, 1995, 1996
III (2000s)	2003, 2004, 2005, 2008, 2009
IV (2010s)	2013, 2014, 2016, 2018

2.3 Results

2.3.1 MESMA library and fractions

The final endmember library was processed based on the criteria described in Section 2.2.3.2 and included two GV (one reference, GV1, and one image, GV2) endmember, two NPV (one reference, NPV1, and one image, NPV2) endmember, and three Soil (two reference Soil2 and Soil3, and one image, Soil1) endmember spectra (Fig. 2-2). The allowed models consist of all possible permutations of the endmember types listed in Table 2-4, resulting in 7 two-endmember models, 16 three-endmember models and 12 four-endmember models.

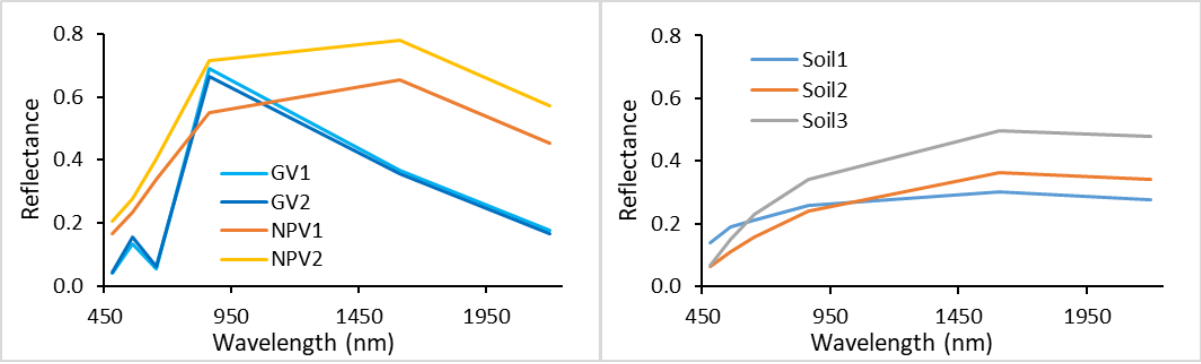

Figure 2-2: Spectra included in the final endmember library

MESMA results without shade normalization are shown in Fig. 2-3. Water, cloud and shadow are mostly unmodeled and appear black in the map. The park and its buffer zone community forests are dominated by green vegetation, which include highland Sal forests, riverine forests, and riparian grasslands (Fig. 2-3). Sal forests account for the majority of the green vegetation in the study area, and they appear darker in the map than the latter two vegetation types. NPV and Soil pure pixels are rare and their fractions mostly concentrate in riverine habitats, including gravels fields, river banks and senesced grasses. The landscape is observed to be relatively uniform within the study area compared to outside human settlements surrounded by the Narayani and Rapti Rivers, where human settlements and agricultural lands prevail (Fig. 2-1). MESMA fraction validation produces similar ranges of accuracy for GV (R^2 = 0.95), NPV (R^2 = 0.92) and Soil (R^2 = 0.93), indicating good MESMA results (Fig. 2-4).

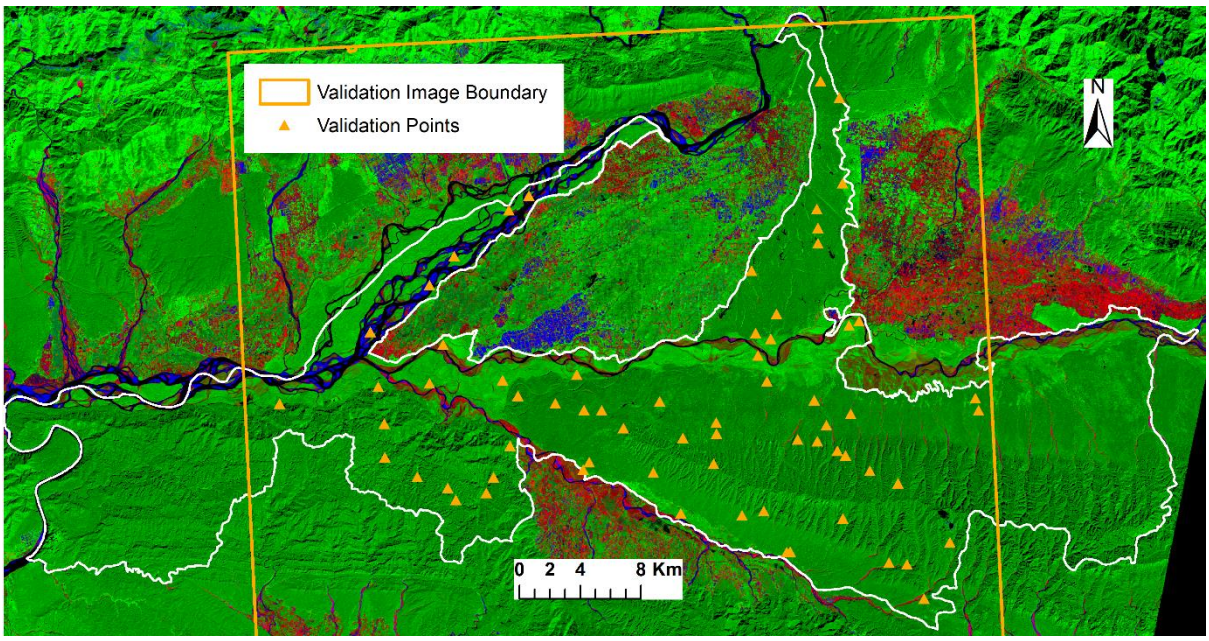

Figure 2-3: False color three band composite of MESMA results with CNP and buffer zone boundaries highlighted (white polygon). Image acquisition date: 27 October 2014. Red: NPV; Green: GV; Blue: Soil; Black: water, cloud, cloud shadow or no data. The southern boundary of the validation image extends beyond this figure extent.

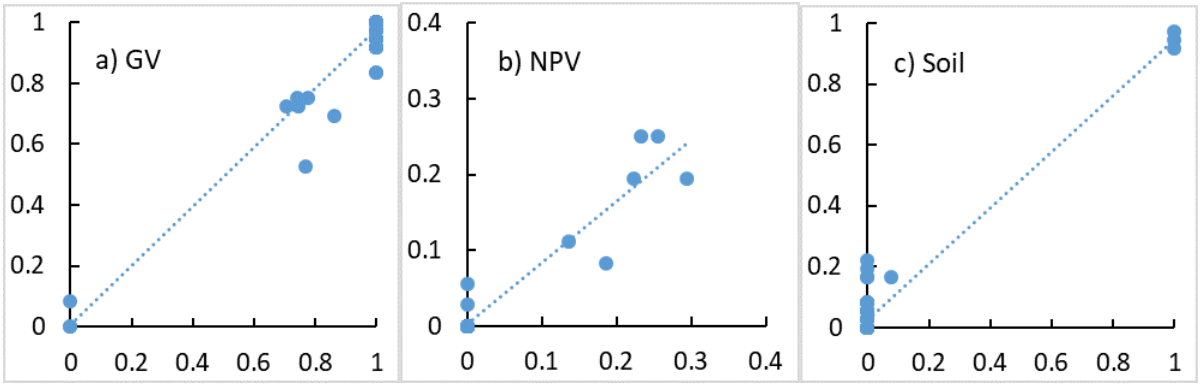

Figure 2-4: Scatterplots of MESMA fraction validations. Y axis is the MESMA fractions and X axis is the reference fractions.

2.3.2 Water coverage in community forests

Water coverage within the 21 community forests in the study area varies dramatically (Fig. 2-5 & Table 2-6). The four East Sal forests (BAND, NABA, DASH and BATU) and two inland South West Rapti forests (MALI and RADH) have minimal water fractions throughout the study period. Rivers and ponds account for the few water fractions in NABA, DASH and BATU, whereas BAND, MALI and RADH are completely water-free.

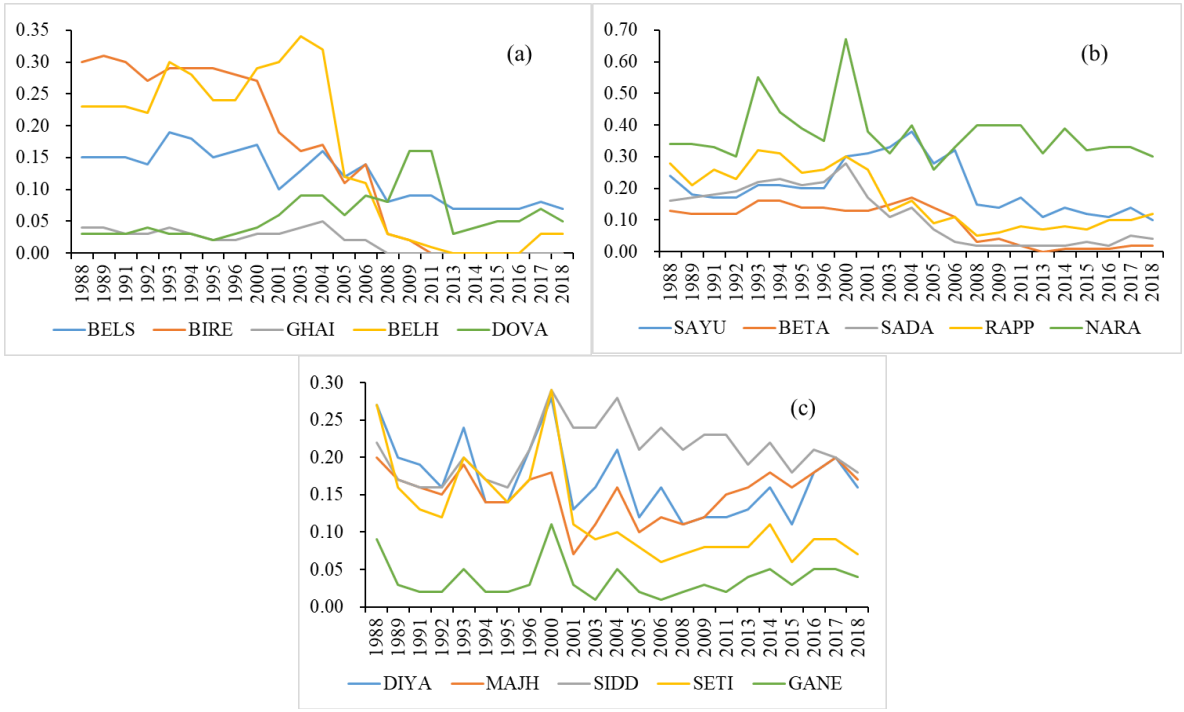

Figure 2-5: Water fractions in (a) South Central Rapti, (b) South West Rapti (excluding MALI and RADH) and Far West, as well as (c) North Narayani community forests from 1988 to 2018.

Table 2-6: Average water fractions of each community forest from 1988 to 2018

Group	Forest	Water
East Sal	BAND	0.00
	NABA	0.00
	DASH	0.01
	BATU	0.00
South Central Rapti	BELS	0.12
	BIRE	0.15
	GHAI	0.02
	BELH	0.16
	DOVA	0.06
South West Rapti	SAYU	0.20
	BETA	0.09
	MALI	0.00
	RADH	0.04
	SADA	0.11
Far West	RAPP	0.17
	NARA	0.37
North Narayani	DIYA	0.17
	MAJH	0.15
	SIDD	0.21
	SETI	0.12
	GANE	0.04

The remaining 15 forests are all riverine and their fluctuations in water fractions reflect the historical changes in river channels. In South Central Rapti forests, the Rapti River used to wand around the southern border of BELS but has been cutting through it since 2001. The river has also diverged to the south of BELH and SADA since 2005. The Narayani River flows right through NARA, leaving it with the highest water coverage among all forests. The five North Narayani forests (DIYA, MAJH, SIDD, SETI and GANE) remain relatively stable to the south of the river main course.

2.3.2 Water-adjusted green vegetation fractions

The four East Sal forests have minimal disturbances from flooding or river channel changes and have the highest average green vegetation fractions (0.65~0.79) among all forests (Fig. 2-6 & Table 2-7). Especially for recent years, the green vegetation fractions are all around

or above 0.95. MALI in the South West Rapti group and GANE in the North Narayani group also have relatively high average green vegetation fractions (0.74 and 0.68, respectively). Highly disturbed by the river flows, SAYU from the South West Rapti group and NARA from the Far West group have the lowest average green vegetation fractions (0.20 and 0.21, respectively) among all forests.

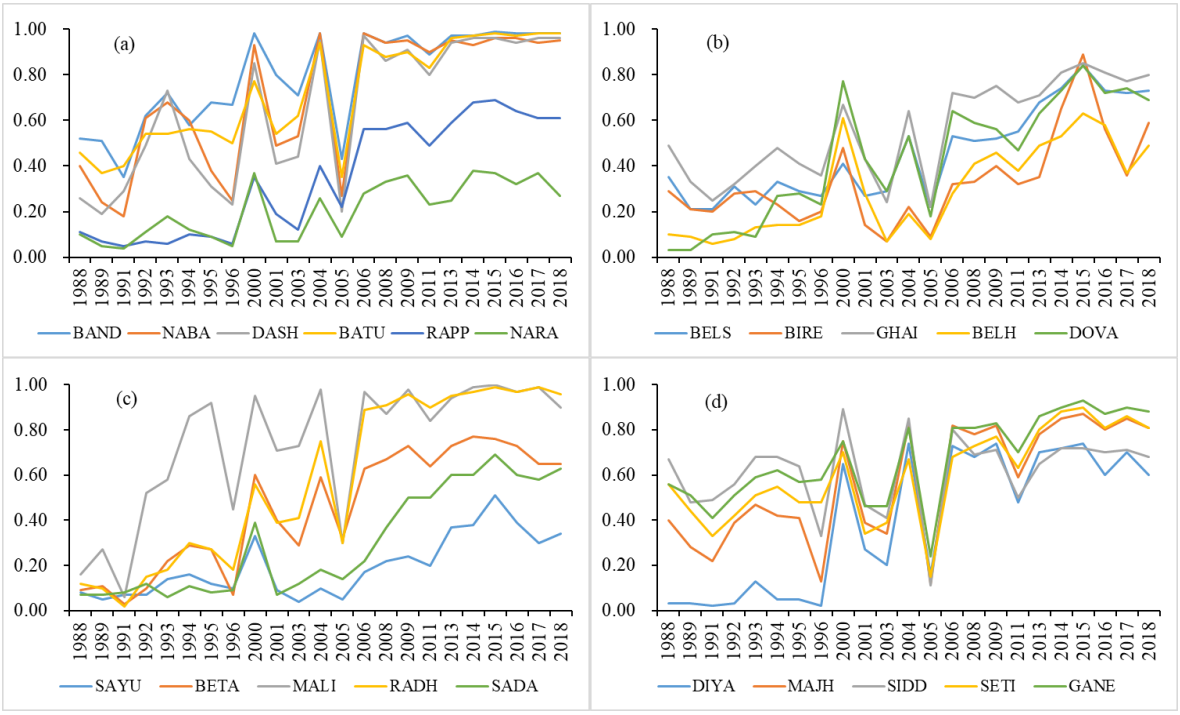

Figure 2-6: Water-adjusted green vegetation fractions of (a) East Sal and Far West, (b) South Central Rapti, (c) South West Rapti and (d) North Narayani community forests from 1988 to 2018.

Table 2-7: Average water-adjusted green vegetation fraction of each forest from 1988 to 2018

Group	Forest	Water-adjusted GV
East Sal	BAND	0.79
	NABA	0.70
	DASH	0.65
	BATU	0.72
South Central Rapti	BELS	0.46
	BIRE	0.33
	GHAI	0.56
	BELH	0.29
	DOVA	0.43
South West Rapti	SAYU	0.20
	BETA	0.45
	MALI	0.74
	RADH	0.57
	SADA	0.30
Far West	RAPP	0.34
	NARA	0.21
North Narayani	DIYA	0.39
	MAJH	0.57
	SIDD	0.61
	SETI	0.60
	GANE	0.68

Despite occasional spikes and valleys largely due to image capture dates, the general trends of the green vegetation fraction curve are ascending (Fig. 2-6). We examine their statistical significances in Section 2.3.4.

2.3.3 Water-adjusted NDFI

NDFI is a useful indicator of deforestation and forest degradation, with value 1 indicating compact forest canopies (Souza Jr. et al., 2005). NDFI accentuates the degradation signals by combining multiple impacts of forest degradation, including an increase in NPV and increase in bare soil. In the community forests, the general patterns of NDFI are similar to those of green vegetation fractions (Fig. 2-7 & Table 2-8). The four East Sal forests, plus MALI and GANE, have relatively high average NDFI values (0.43~0.67). The NDFI values of NARA and SAYU (-0.54 and -0.43, respectively) are lower than other forests. The general trends of NDFI curves

are generally ascending. The statistical significances of NDFI dynamics will also be examined in Section 2.3.4.

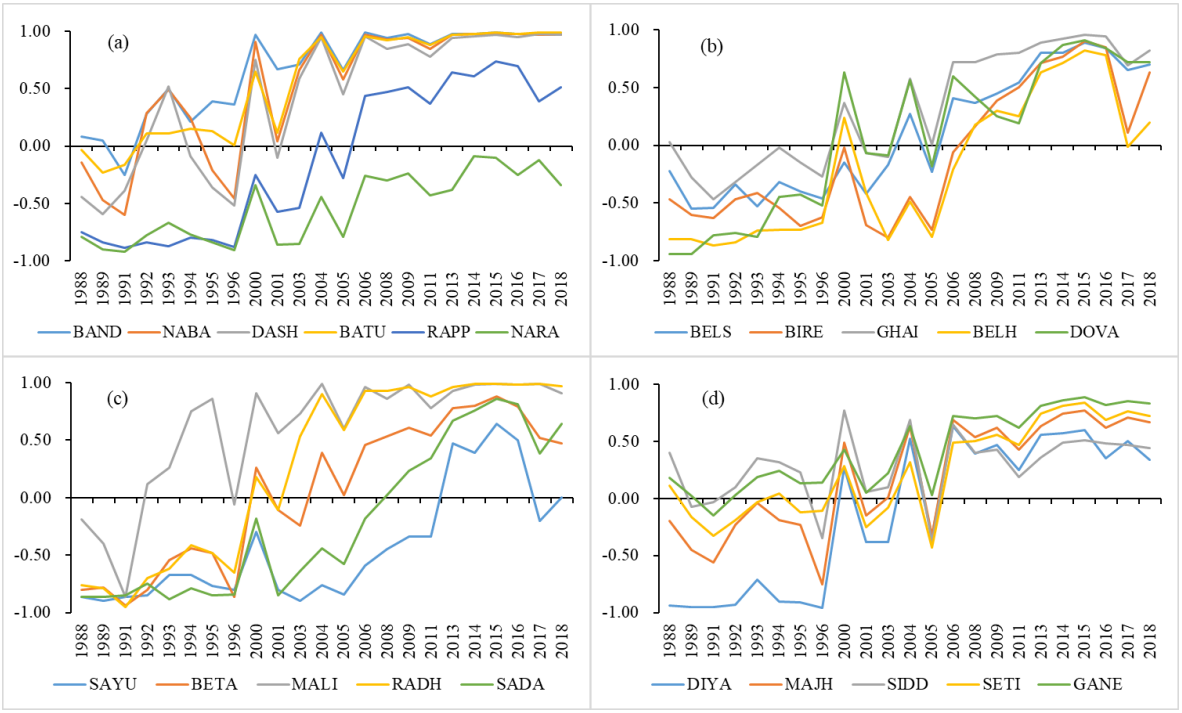

Figure 2-7: NDFI of (a) East Sal and Far West, (b) South Central Rapti, (c) South West Rapti and (d) North Narayani community forests from 1988 to 2018.

Table 2-8: Average NDFI of each forest from 1988 to 2018

Group	Forest	NDFI
East Sal	BAND	0.67
	NABA	0.52
	DASH	0.44
	BATU	0.56
South Central Rapti	BELS	0.11
	BIRE	-0.09
	GHAI	0.32
	BELH	-0.21
	DOVA	0.06
South West Rapti	SAYU	-0.43
	BETA	0.05
	MALI	0.59
	RADH	0.27
	SADA	-0.21
Far West	RAPP	-0.12
	NARA	-0.54
North Narayani	DIYA	-0.13
	MAJH	0.19
	SIDD	0.29
	SETI	0.25
	GANE	0.43

2.3.4 Community forest dynamics

2.3.4.1 Water-adjusted green vegetation fractions

Comparisons among different periods indicate the trends of change in green vegetation fractions in the forests (Table 2-9). Only one significant change (BIRE between Periods I and II) shows a decrease in green vegetation fractions, whereas all other changes show increases. Five forests (BELH, DOVA, MALI, RADH and GANE) rapidly greened-up after the establishments of the community forests in the 1990s (Period I vs. Period II). Comparing Period I (before the 1993 Community Forestry Act) with Period IV (2010s), all forests show significant increases in green vegetation fractions. Combining all values after 1993 into a single dataset and comparing between Period II~IV with Periods I, the null hypothesis (later period has no higher values than the previous period) cannot be rejected for only two forests (BIRE

and SIDD). The green-up signals are highly correlated with the establishment of the community forests.

Table 2-9: Comparison of green vegetation fractions among different periods. Only significant p values (<0.05) are listed. Italic numbers (BIRE, I vs. II) indicate decreases. All others indicate increases. Period I: Pre 1993; Period II: 1994-1999; Period III: 2000s and Period IV: 2010s.

Group	**Forest**	I vs. II	II vs. III	III vs. IV	I vs. III	II vs. IV	I vs. IV	I vs. II~IV
East Sal	BAND				3.77E-02	4.22E-03	1.07E-03	3.19E-03
	NABA					1.77E-02	3.17E-03	2.20E-02
	DASH		4.19E-02			4.41E-03	2.26E-03	2.80E-02
	BATU				3.08E-02	1.07E-03	6.47E-05	4.98E-04
South Central Rapti	BELS			5.50E-03	4.70E-02	3.89E-06	3.86E-06	1.83E-03
	BIRE	*4.83E-02*		5.14E-03		7.51E-03	6.75E-03	
	GHAI			4.02E-02		4.18E-04	4.79E-05	6.01E-03
	BELH	7.12E-03		1.05E-02		1.22E-05	5.17E-06	1.19E-03
	DOVA	8.18E-05		1.35E-02	6.28E-03	7.45E-06	3.30E-07	1.11E-05
South West Rapti	SAYU			1.18E-03		7.32E-04	7.58E-07	4.65E-03
	BETA		1.70E-02	4.37E-02	3.99E-03	2.92E-03	5.64E-07	6.65E-05
	MALI	3.91E-02			1.18E-02		1.73E-03	1.46E-03
	RADH	1.97E-02	1.38E-02	4.48E-02	7.38E-03	1.24E-03	2.86E-06	2.86E-06
	SADA		4.45E-02	5.09E-03	3.84E-02	3.77E-08	8.05E-10	1.63E-03
Far West	RAPP		1.69E-02	2.77E-02	1.53E-02	9.23E-07	8.05E-07	6.22E-04
	NARA		4.42E-02			6.99E-04	4.03E-04	7.41E-03
North Narayani	DIYA		1.24E-02		1.35E-02	2.37E-05	8.10E-06	5.44E-04
	MAJH					1.91E-02	1.09E-04	1.16E-02
	SIDD						2.91E-02	
	SETI			3.78E-02		2.11E-04	1.73E-04	1.72E-02
	GANE	3.70E-02				2.53E-04	1.60E-04	7.50E-03

2.3.4.2 NDFI

The change patterns of NDFI for all community forests are similar to those of green vegetation fractions (Table 2-10), only that no significant decreases are detected. Three forests (BELH, DOVA and RADH) show rapid greening-up after the establishment of community forests (Period I vs. Period II). All comparisons between Periods I and IV indicate significant increases. Except for SIDD, all other comparisons between Period I and Periods II~IV show prominent green-up signals.

Table 2-10: Comparison of NDFI among different periods. Only significant p values (<0.05) are shown. All values indicate increases in NDFI. Period I: Pre 1993; Period II: 1994-1999; Period III: 2000s and Period IV: 2010s.

Group	Forest	I vs. II	II vs. III	III vs. IV	I vs. III	II vs. IV	I vs. IV	I vs. II~IV
East Sal	BAND		4.78E-04		1.16E-03	3.50E-03	1.22E-03	1.54E-03
	NABA		1.18E-02		5.15E-03	1.66E-02	3.60E-03	1.17E-02
	DASH		1.20E-03	4.81E-02	3.29E-03	4.63E-03	2.61E-03	1.10E-02
	BATU		3.48E-05		6.43E-06	1.38E-03	6.64E-05	2.13E-05
South Central Rapti	BELS		7.75E-03	5.53E-03	5.07E-03	9.64E-06	1.34E-06	5.44E-04
	BIRE			6.86E-03		2.14E-06	9.27E-08	1.46E-02
	GHAI		2.00E-02	2.98E-02	9.71E-03	4.22E-04	2.39E-05	4.50E-04
	BELH	9.17E-03		7.68E-03		1.11E-03	8.87E-04	1.70E-03
	DOVA	1.22E-04	5.23E-03	5.07E-03	4.65E-04	8.29E-07	7.73E-09	1.11E-05
South West Rapti	SAYU			2.12E-04		4.22E-04	3.26E-04	6.17E-03
	BETA		3.21E-03	2.30E-02	9.69E-04	1.77E-03	3.66E-06	4.56E-05
	MALI				2.17E-03		2.12E-03	1.73E-03
	RADH	2.50E-02	1.56E-05		3.28E-06	1.17E-03	2.83E-06	8.13E-06
	SADA		1.78E-02	2.46E-03	1.67E-02	1.89E-06	1.82E-07	1.38E-03
Far West	RAPP		6.39E-03	2.84E-02	6.34E-03	3.00E-07	3.16E-07	3.78E-04
	NARA		3.18E-02		4.25E-02	3.25E-04	2.29E-04	3.86E-03
North Narayani	DIYA		3.20E-03		3.77E-03	1.64E-05	1.31E-06	2.69E-04
	MAJH		2.10E-02		1.65E-02	1.44E-02	8.58E-05	3.50E-03
	SIDD						1.57E-02	
	SETI			2.01E-02		3.98E-04	5.97E-05	5.01E-03
	GANE			2.96E-02	2.22E-02	1.40E-03	1.20E-04	4.96E-04

2.4 Discussion

Situated in the frontier of human-environment interactions, the western Chitwan community forests provide perfect opportunities to study how human and endangered large carnivores and ungulates can coexist at fine spatial scales (Carter et al., 2012). The vegetation conditions of these forests are vital to both the survival of the endangered species and the livelihoods of local residents. To date, however, there have been no systematic assessments of these forests for the past three decades. This chapter adopts two indicators (green vegetation fraction from MESMA and NDFI) to evaluate the vegetation dynamics in these forests and adjusts them to minimize influences from water bodies.

Although the green vegetation fractions and NDFI values have been increasing during the 30 years, and the values for post-1993 imagery are significantly higher than that of the pre-1993 imagery, factors other than the community forest management may also have affected the

green-up signals in the study area. Since the late 1990s, a notorious exotic plant, *M. micrantha*, nicknamed “mile-a-minute-vine”, has been invading the Chitwan National Park and its buffer zone (Murphy et al., 2013). The invasion is most prominent in the riparian habitats, affecting all riverine community forests in this study (Dai et al., 2020). As an understory creeping vine, *M. micrantha* tends to fill the gaps between forest canopies and increase green vegetation fractions in the forest image pixels. In other words, in addition to reforestation, the invasion may also have contributed to the green-up signals quantified in this chapter.

Even though it is not the ultimate objective of this chapter to articulate the relative contributions to the green-up signals, from the most conservative perspective, at least in the East Sal forests where invasion has been minimal, community forestry management and reforestation has been the prime cause for green-up. Besides, in the five forests (BELH, DOVA, MALI, RADH and GANE) where green vegetation fractions significantly increased in the years right after 1993, the contribution of reforestation appears to be the main reason for green-up, since the invasion of *M. micrantha* was minimal back then.

2.5 Conclusions

The green vegetation dynamics in Chitwan community forests, Nepal from 1988 to 2018 is evaluated in this chapter. The comparison of green vegetation fractions from spectral mixture analysis and a forest degradation index (NDFI), based on two-sample unequal variance T-tests, show that the forests have been continually greened-up during those thirty years. Although the invasion of an understory vine may have partially contributed to the green-up signals in some forests, the establishment of community forests and the resultant forest managements should be credited for some of the green-up signals, especially in the inland Sal forests. Future work

may be conducted to quantify and separate the relative contributions of exotic plant invasion and community forest management practices, especially in the riverine forests where invasion has been most prominent.

3. Chapter III: Mapping understory invasive plant species with field and remotely sensed data in Chitwan, Nepal

3.1 Introduction

Invasive species have long been associated with human-introduced environmental change, rendering negative effects on ecosystem services and human well-being (Pejchar & Mooney, 2009). The first step in invasive species management and intervention requires identifying their geographical locations. Traditional invasive plant detection and identification usually involves intensive field surveys, which can be time consuming and expensive. Remote sensing provides a potential alternative method for detection. In general, direct remote sensing of invasive plants aims to detect spectral, textural and/or phenological differences between the invasive and native species (Bradley 2014). Spectral differentiation focuses on the unique spectral signatures of invasive plants compared to native vegetation and is mostly applied to hyperspectral imagery (Asner et al., 2008; Barbosa et al., 2016; Underwood et al., 2003). Textural differentiation examines the distinct spatial patterns of invasive species and background land covers captured within a neighborhood of adjacent pixels and is usually conducted with high-spatial resolution imagery, depending on the size of the invasive plant or its aggregation (Lishawa et al., 2013; McCormick 1999; Pearlstine et al., 2005). Phenological differentiation identifies different seasonal or inter-annual growth patterns between invasive and native plants, including base and maximum level greenness of growing season, time and rate of greening up and senescence, date of the middle of the season, and other parameters (Bradley et al., 2018; Hoyos et al., 2010; Peterson 2005; Somers & Asner, 2013). Phenological differentiation requires repeat imaging to gain adequate temporal information to define spectral differences.

Obscured by the top canopy, detection of understory invasive plants is even more challenging, especially in closed-canopy mature forests. Direct detection through passive optical remote sensing techniques can be achieved when understory vegetation has distinct phenologies from overstory species, such as an extended green season or earlier greening up when the overstory trees are leaf-off (Taylor et al., 2013; Tuanmu et al., 2010; Wilfong et al., 2009). Understory invasive plants may be indirectly identified if the invasion introduces competition for nutrients as well as water and renders biochemical changes in overstory leaves, thus altering the spectral features of the overstory vegetation (Asner & Vitousek, 2005). Indirect detection of understory invasive plants may also be achieved through linking its presence with remote sensing imagery related biophysical and socio-ecological factors governing its growth, such as light-availability and human disturbance in the forests (Joshi et al., 2006).

Spectral mixture analysis (SMA) is a powerful tool for inspecting mixed pixels in remote sensing imagery and quantifying their constituents, especially for moderate and coarse spatial resolution images. Theoretically, the invasion of understory plants can introduce changes to the types and quantities of constituents within mixed pixels, which may be directly or indirectly detected in SMA. Nevertheless, few studies have incorporated SMA to investigate understory invasive plant mapping. This chapter explores the detection and mapping of understory invasive plant species through multiple endmember SMA (MESMA; Roberts et al., 1998) and maximum entropy (Maxent; Philips et al., 2006) modeling framework. In particular, the spatial extent of *Mikania micrantha* is mapped in Chitwan National Park (CNP), Nepal and its buffer zone community forests. *M. micrantha* is one of the world's most notorious invaders (IUCN

2020) and its invasion is jeopardizing forests and has the potential of totally disrupting local coupled human and natural systems. *M. micrantha* also decreases forest productivity by hindering the growth of native species, weakens social organizations that manage and shape households' resource use in the community forests, and downgrades local ecosystems and their corresponding services (Murphy et al. 2013). According to research literature, and discussions with local forest users and park rangers, *M. micrantha* mostly flourishes in riverine habitats and tends not to grow in higher-elevation environments (Murphy et al. 2013). Given this general distribution pattern, the goal of this chapter is to create a detailed, pixel-based distribution map for *M. micrantha* in the study area. The results from this chapter will help identify the locations of *M. micrantha* and guide local invasive plant species management and intervention practices.

3.2 Methodology

3.2.1 Study area

The study area of this chapter is the Chitwan National Park and its buffer zone community forests (Fig. 3-1). Detailed information on local temperature and precipitation, as well as the vegetation species composition in the forests can be found in Chapter I and Section 2.2.1 of Chapter II.

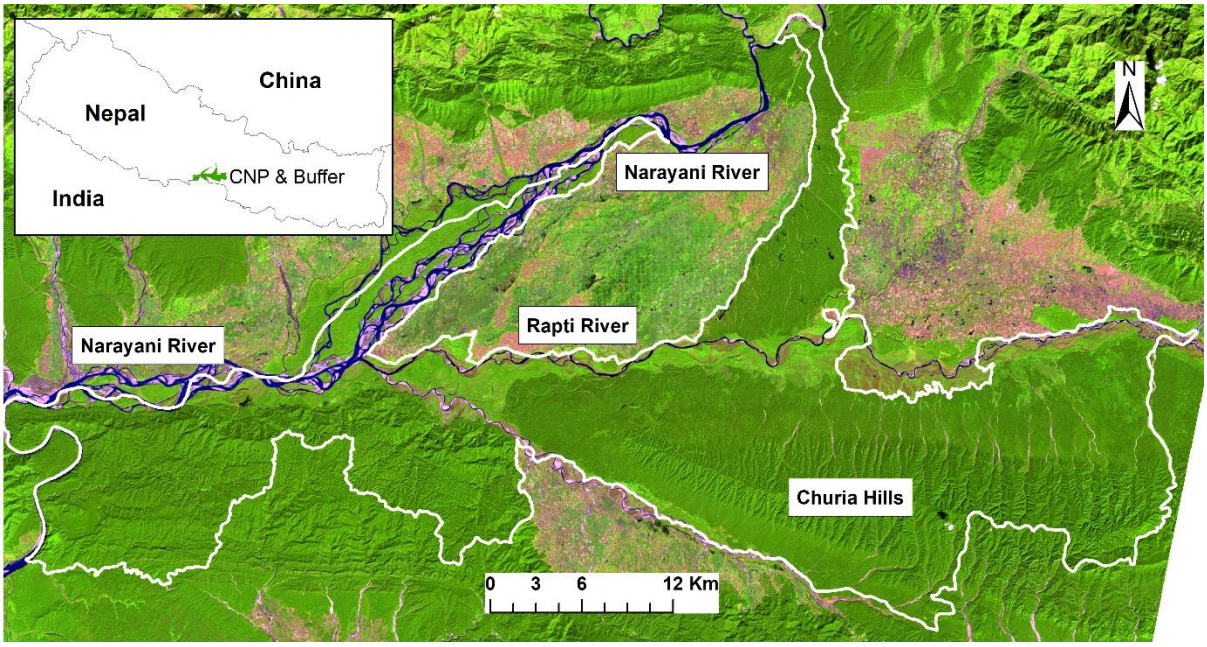

Figure 3-1: False color Landsat 8 three-band composite of the study area (highlighted in white polygon). Image acquisition date: 27 October 2014. Red: Band 6 (1560-1660 nm); Green: Band 5 (845-885 nm); Blue: Band 4 (630-680 nm).

3.2.2 Field vegetation inventory

In the three consecutive years of 2013, 2014 and 2015, field vegetation surveys were conducted in the western Chitwan buffer zone community forests, bounded to the south by the Rapti River and the west by the Narayani River (Fig. 3-2). Field data were collected around the peak biomass period right after the monsoon season, approximately between late September and mid-November. In every community forest, parallel transects were set up that are 200 m apart, angling from human settlements toward the park. Along each transect, at 50 m intervals, a sample site was established with two 5 m by 5 m plots adjacent to each other and perpendicular to the transect. For each plot, several ecological measurements were obtained, including *M. micrantha* coverage (in categories 0-4 through visual estimation, where 0 represents absence of *M. micrantha*, 1 for 1%-25% coverage and 2 for 26%-50% coverage, etc.), canopy cover (in percentage, measured through a forest densiometer) and identification

of dominant tree and herbaceous species.

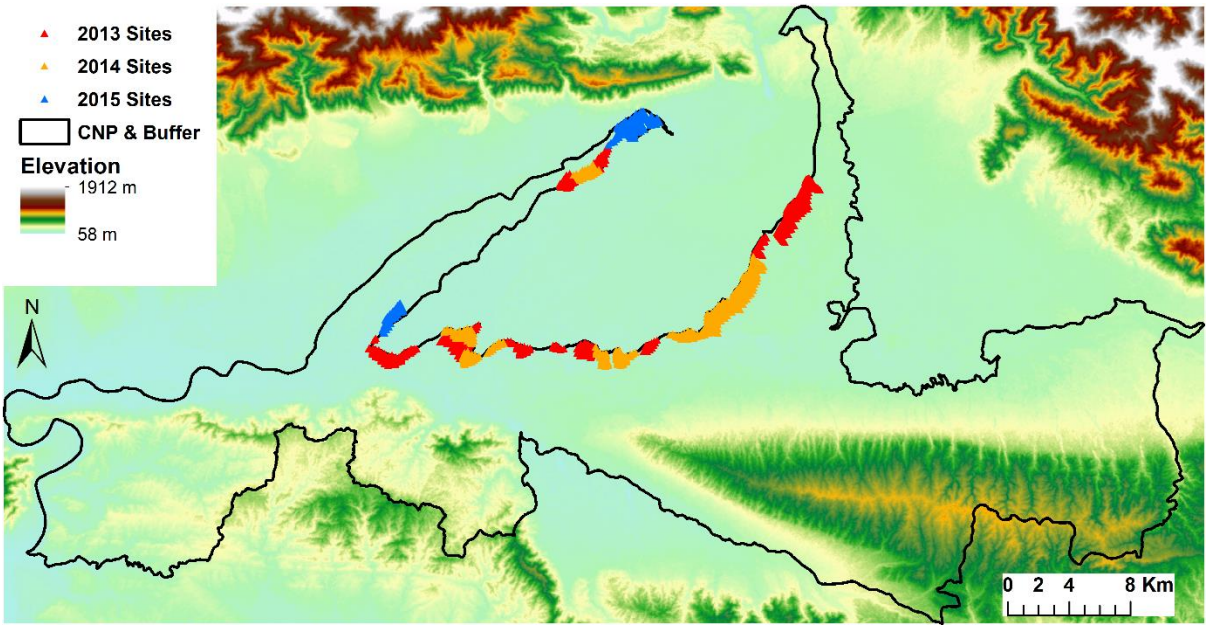

Figure 3-2: Terrain map of the study area and vegetation survey sites.

In the field vegetation survey, the coverage of sample sites in the community forests was affected by accessibility (rivers, lakes and wetlands were inaccessible) and occasionally by likely presence of dangerous animals such as tigers and rhinos. The field vegetation survey team were able to investigate most of the areas to the north of the Rapti River and to the south of the Narayani River (e.g. in BELS, SAYU, NARA, DIYA, MAJH, SIDD and SETI; Fig. 3-3). The team also crossed the borders of three Sal community forests in the east (e.g. BAND, NABA and DASH; Fig. 3-3) and doubled the lengths of the sampling transects.

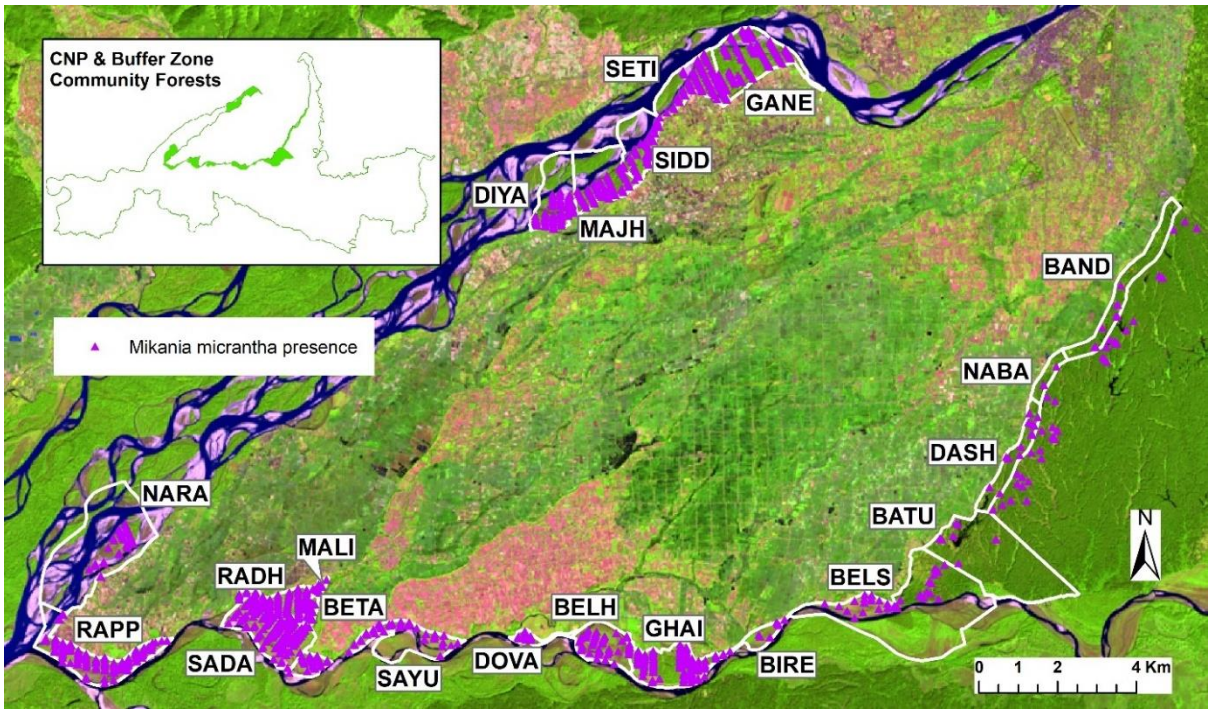

Figure 3-3: Community forests (highlighted by white polygons) in the study area and sample sites with M. micrantha presence. Background image: false color Landsat 8 three-band composite. Image acquisition date: 27 October 2014. Red: Band 6 (1560-1660 nm); Green: Band 5 (845-885 nm); Blue: Band 4 (630-680 nm).

3.2.3 Ground reference spectra

In September 2018, apart from the field vegetation surveys, *in situ* reference spectra were collected for major herbaceous species (including *M. micrantha*) in the community forests. Consult Section 2.2.2 of Chapter II for details on ground reference data collection and processing.

3.2.4 Remotely sensed data

Landsat Operational Land Imager (OLI) surface reflectance products (Level-2) were obtained from USGS EarthExplorer (https://earthexplorer.usgs.gov/) to align with the field vegetation survey dates. For the years 2013, 2014 and 2015, one desirable scene was identified for each year (Path/Row: 142/41; Table 3.1). Also obtained was a 30 m spatial resolution digital elevation model (DEM) derived from Terra Advanced Spaceborne Thermal emission and

Reflectance Radiometer (ASTER) stereoscopic imagery for the study area (NASA/METI, 2019).

Table 3-1: Selected Landsat OLI imagery

Year	Acquisition Date	Cloud Cover	Image Quality
2013	11/09	2.00%	9
2014	10/27	0.94%	9
2015	10/14	4.84%	9

3.2.5 Multiple Endmember Spectral Mixture Analysis

Spectral mixture analysis (SMA) is a classic method for estimating mixed constituents within ground resolution elements associated with image pixels. It assumes that the spectral reflectance of a pixel can be modeled as the weighted sum of endmember reflectance, or spectrally "pure" materials, within that pixel. Most SMA adopts a linear addition method and the weights correspond to fractions of endmembers in the pixel. As an extension of simple SMA, Multiple Endmember SMA (MESMA) allows the number and types of endmembers to vary on a per-pixel basis, generating more legitimate unmixing results for imagery with high inter- and intra-endmember variance (Roberts et al., 1998). This chapter is characterized by adopting the MESMA procedures and results from the Chapter II. MESMA fractions validations can also be found in Chapter II of this dissertation.

For Landsat multispectral imagery of vegetated landscapes, most pixels can be modeled as GV-NPV-Soil-Shade mixture in MESMA. In the study area, *M. micrantha* is genetically and physiologically distinct from other plants, including the other two major invasive species, *Chromolaena odorata* and *Lantana camara*. *M. micrantha* is a perennial creeping vine with higher spectral reflectance than mature forests in the near-infrared wavelength, tends to form dense layers and fill the gaps among top canopies. The hypothesis is that the pixels representing

areas invaded by *M. micrantha* will yield higher GV fractions and lower Shade fractions than unaffected pixels. To test this hypothesis, two-sample T-tests (two-tailed and unequal variance) were conducted for both GV and Shade fraction values between presence and background pixels to identify potential significant differences.

3.2.6 Maximum Entropy Modeling Framework

In this chapter, the software package Maxent was utilized to generate models for mapping *M. micrantha* distribution in the Landsat image we selected (Philips et al., 2006). Maxent makes presence predictions based on the relationships between presence records and corresponding environmental data. The difference between Maxent and many other species distributions modeling methods is that there is no real "absence data" in the modeling procedures, and it is typically developed to accommodate presence-only data. In the vegetation survey mentioned earlier in this chapter, the presence and coverage of *M. micrantha* were recorded for all 5 m by 5 m sample plots. If *M. micrantha* was not detected in a specific sample plot, it cannot be guaranteed if it was absent from the whole 30 m by 30 m Landsat ground resolution element, or whether the plant was present in that element but outside of the sample plots. Therefore, instead of interpreting the field records as "presence-absence" data, they should be more appropriately treated as "presence-only" data.

This chapter also emphasizes the importance of the representativeness of presence data to Maxent model results. The ultimate objective of Maxent is to make predictions of species distributions by evaluating the presence records and their corresponding environmental information, and the representativeness of any presence data is vital to the overall model accuracy. Ideal presence records should include all types of possible presence locations (in the

dimensions of the environment data) in the target predicting area. In this chapter, although the community forests and sample sites are spatially biased, residing mostly on the fringe of the park and covering relatively small areas compared to the whole study area, they are highly diverse in floral species and contained all local vegetation types (e.g. Sal forest, riverine forest and riparian grassland), and consequently contain all possible *M. micrantha* presence location types. Because the general distribution pattern of *M. micrantha* in the study area (mostly in riverine habitats) are already known, the sampling data can be considered sufficient.

In the Maxent models, pixels with *M. micrantha* coverage level of 1 or above (excluding all pixels without detected coverage) were adopted as presence data; 10000 pixels were randomly selected from the study area as background data (Phillips & Dudik, 2008). The four fraction layers (GV, NPV, Soil and Shade, from MESMA) and elevation were imported as potential predictor variables. The maximum iterations were set at 500 times and the predicted *M. micrantha* presence probabilities were averaged for each pixel. The presence data and MESMA fraction layers could only account for the ground conditions around the time the records and imagery were collected, thus for each year (2013, 2014 and 2015), one map was generated for each predictor combination (e.g. GV-Shade-NPV, GV-Shade-Soil and GV-Shade-DEM).

3.2.7 Model validation

The receiver operating characteristic (ROC) analysis and the area under the ROC curve (AUC) incorporated in Maxent were used for model evaluation (Fielding & Bell, 1997; Pearce & Ferrier, 2000). In general, AUC values between 0.7 and 0.8 indicate fair modeling results, values between 0.8 and 0.9 are considered good, and values higher than 0.9 are excellent

(Fielding & Bell, 1997; Pearce & Ferrier, 2000). In this chapter, among all the presence data, 75% of them were randomly allocated for model training, and the remaining 25% for testing. Kappa analysis was also applied to evaluate Maxent results (Cohen 1960). For this purpose, 100 presence pixels and another 100 background pixels were randomly selected from the whole study area in each year's modeling results. Continuous presence probabilities were dichotomized to 0 or 1, with values greater than 0.5 assigned to the latter. Since all pixels, including presence data, were involved in the random selection of background data, the AUC and kappa values tended to be underestimated in this case. Jackknife analyses were conducted to evaluate the relative contributions of the environmental variables. The results would be the AUC values of the relative Maxent model if only one of the variables was included in the modeling process (e.g. GV-only or Shade-only Maxent models, etc.).

3.3 Results

3.3.1 *M. micrantha* presence in the sample sites

The fieldwork was conducted in the two-month window right after the monsoon and it took us three years (2013-2015) to survey all 21 community forests. The field vegetation survey team were able to visit 2219 sample sites in total, of which 1038 were invaded by *M. micrantha*. The four East Sal forests were sparsely invaded, with *M. micrantha* presence at around 10% of the sample sites (Table 3-2; Fig. 3-3). Invasions were more prominent in riverine forests, where *M. micrantha* occurred in more than half of the sample sites (Table 3-2; Fig. 3-3). This general pattern resembles the results from the assessment of *M. micrantha* distribution conducted in the study area in 2008 (Murphy et al., 2013). Forests in the South West Rapti region and the North Narayani region bore the most severe invasion, with invasion rates close to or above

80%. Two forests in particular, MALI and RADH, had *M. micrantha* detected at every sample site.

Table 3-2: Number of total sample sites and invaded sites in each community forest

Region	Forest Code	Total Sites	Invaded Sites	Invasion %
East Sal	BAND	299	23	7.7%
	NABA	39	4	10.3%
	DASH	232	31	13.4%
	BATU	126	7	5.6%
South Central Rapti	BELS	167	33	19.8%
	BIRE	28	7	25.0%
	GHAI	136	100	73.5%
	BELH	87	39	44.8%
	DOVA	19	10	52.6%
South West Rapti	SAYU	52	21	40.4%
	BETA	109	62	56.9%
	MALI	9	9	100.0%
	RADH	76	76	100.0%
	SADA	177	147	83.1%
Far West	RAPP	148	101	68.2%
	NARA	88	33	37.5%
North Narayani	DIYA	70	62	88.6%
	MAJH	74	67	90.5%
	SIDD	59	47	79.7%
	SETI	92	78	84.8%
	GANE	136	99	72.8%

3.3.2 MESMA fractions

Based on the MESMA results in Chapter II, the 2219 sample sites are used in the community forests to identify potential significant differences in GV and Shade fractions between *M. micrantha* invaded sites (1038) and background sites (1181). T-test results confirm that compared to background pixels, presence pixels generate significantly higher GV fractions and lower Shade fractions (both $p < 0.001$; Figure 3.4).

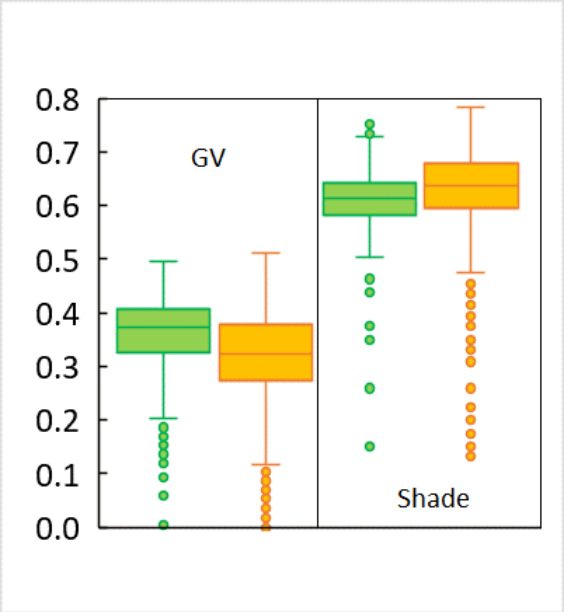

Figure 3-4: Boxplots of GV and Shade fractions between presence (green) and community forest background (orange) pixels.

3.3.3 *M. micrantha* distribution

Incorporating both GV and Shade fraction layers with an addition of NPV or Soil, the AUC values of *M. micrantha* distribution Maxent models for training and testing data are both between 0.74 and 0.86, respectively (Fig. 3-5, first two columns from the left). The relative kappa coefficients range from 0.49 to 0.61. Both ranges, even though underestimated due to the inclusion of presence records in background data, indicate fair or good model results. The estimated *M. micrantha* presence probabilities ranged from 0 to 1 across the study area, with most of the higher probability pixels located in riverine forests and riparian grasslands along the Narayani and Rapti Rivers (Fig. 3-6). Some of the high probabilities were associated with high-GV-fraction pixels at higher elevations, e.g. the sunlit slopes along the southern side of Churia Hills (Fig. 3-6).

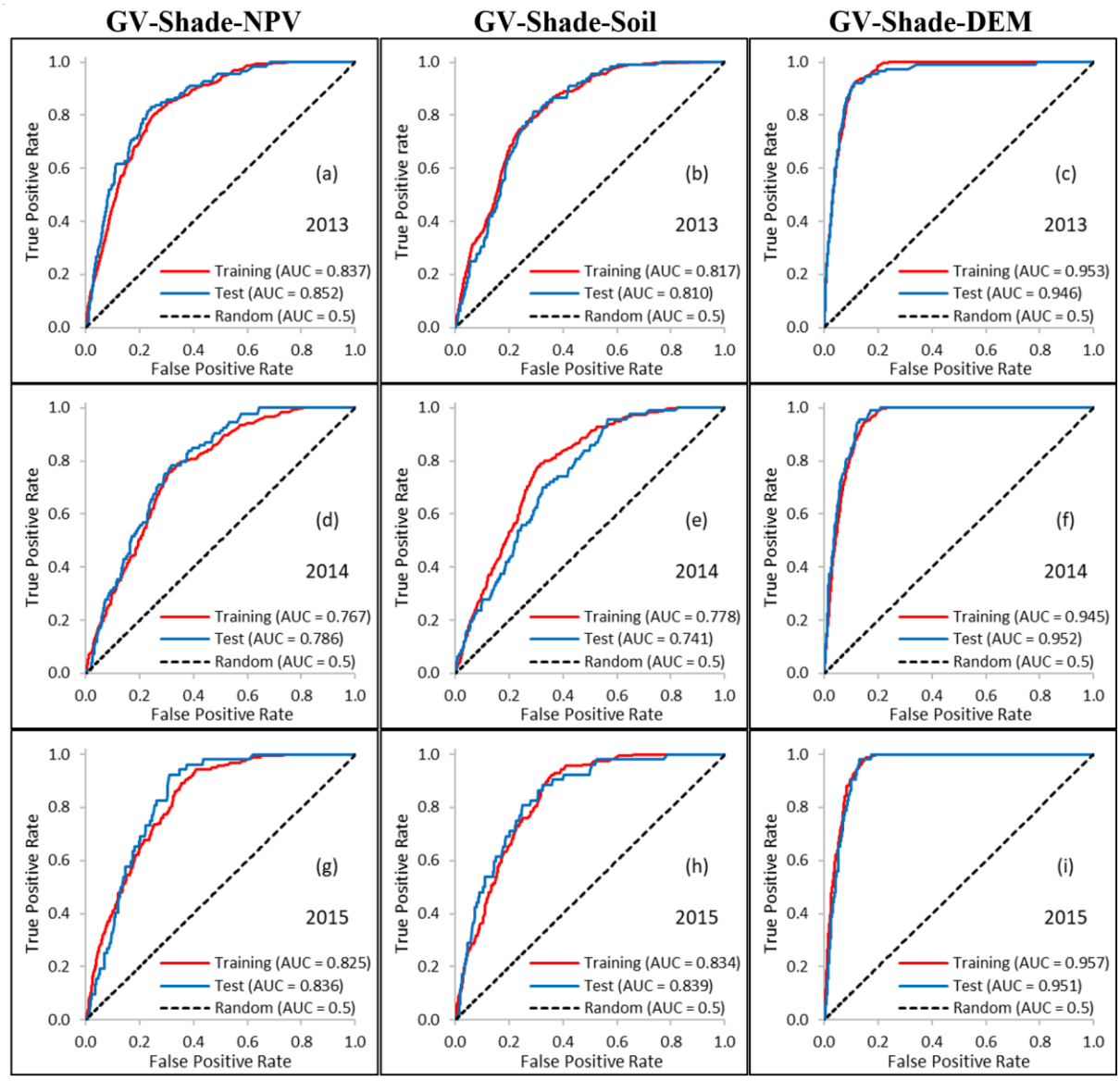

Figure 3-5: ROC curves and AUC values for training and test data in GV-Shade-NPV (first column, a, d, g), GV-Shade-Soil (second column, b, e, h) and GV-Shade-DEM (third column, c, f, i) Maxent models for 2013, 2014 and 2015.

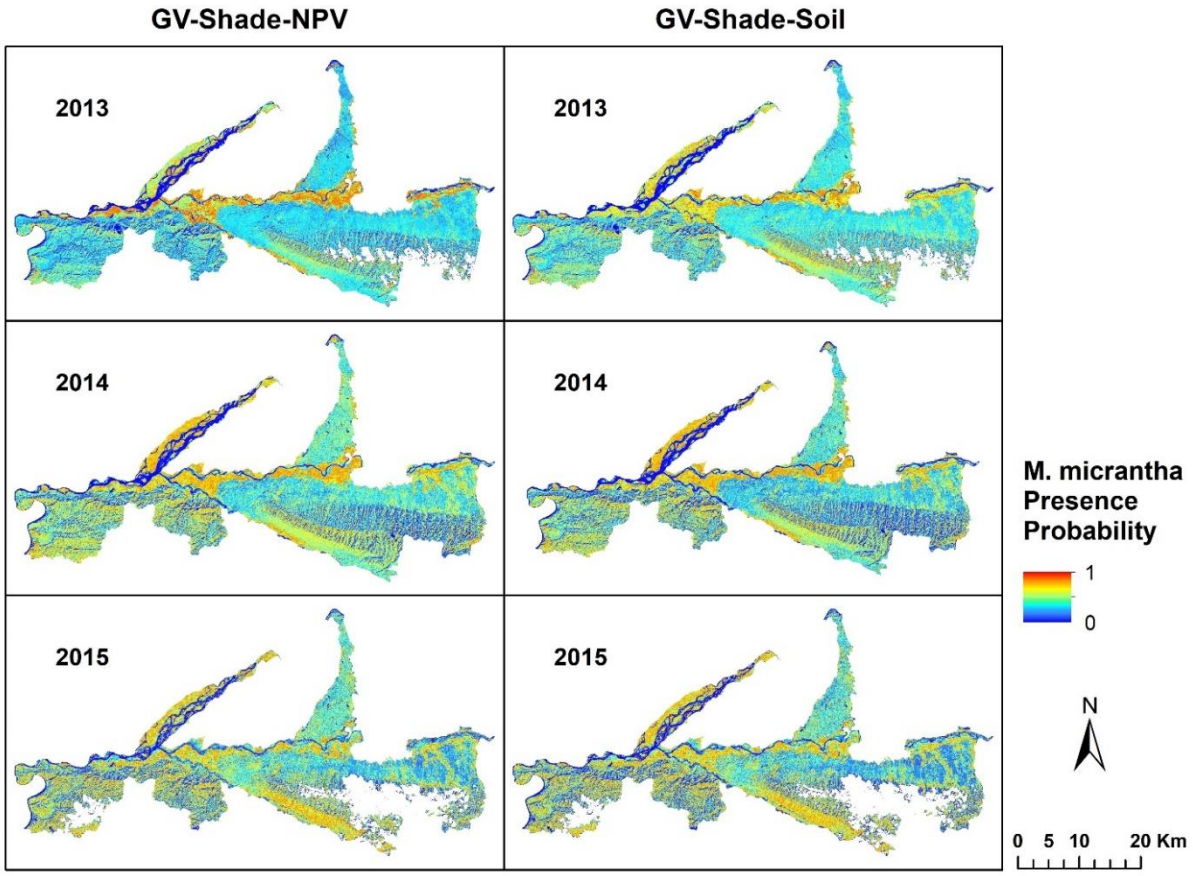

Figure 3-6: M. micrantha average presence probability maps generated from GV-Shade-NPV (First column from left) and GV-Shade-Soil (Second column from left) Maxent models in 2013, 2014 and 2015. Large blue patches above Churia Hills in 2013 and 2015 maps are associated with clouds or cloud shadows.

Although MESMA-fraction-only Maxent models (e.g. GV-Shade-Soil and GV-Shade-NPV) produce fair/good model results (AUC between 0.7 and 0.9, kappa between 0.4 and 0.75), the inclusion of elevation (DEM) as a model input significantly improves map accuracy, with both training and testing AUC values around 0.95 (Fig. 3-5, last column at right). Their kappa coefficients range between 0.75 and 0.81. Both ranges indicate excellent mapping results. The effects of including elevation will be further examined in the Discussion section.

3.4 Discussion

3.4.1 MESMA fractions and *M. micrantha* mapping

In this chapter, an effective approach is developed for mapping understory invasive plant

species using SMA and the Maxent modeling framework. By applying MESMA to Landsat 8 OLI surface reflectance products, this chapter verify the significant differences in GV and Shade fractions between *M. micrantha*-invaded and non-invaded pixels. Then the spatial extent of *M. micrantha* is successfully mapped in Chitwan National Park and the community forests within its buffer zone using MESMA generated fraction layers. The resulting distribution maps prove to be fair/good for MESMA-fraction-only models (AUC between 0.7 and 0.9, kappa between 0.4 and 0.75). The inclusion of elevation as a model input produces excellent map results (AUC above 0.9 and kappa above 0.75). While endmember fractions from MESMA have been used for sub-pixel land cover mapping (Roberts et al., 1998; Powell et al., 2007), deforestation and forest degradation evaluation (Souza Jr. et al., 2005; Souza Jr. et al., 2013) and plant species classification (Roberts et al., 2015; Roth et al., 2015), in this chapter their applications are extended to analyze the spatial extent of invasive plant species growing under forest canopies.

By analyzing endmember fractions generated from MESMA, an important finding arise: pixels with *M. micrantha* invasion can be distinguished from background pixels in the study area. Higher GV fractions and lower Shade fractions reflect the differences between invaded forests and unaffected landscape types. The growth and densification of *M. micrantha* from ground to tree crowns in the forests may contribute to the higher GV fractions, whereas the filling between canopy gaps may account for the lower Shade fractions of the invaded pixels.

Some of the pixels along the southern side of Churia Hills are also assigned high-probability values, especially in the 2015 maps (Fig. 3-6). These results may be explained by the limitation of the 2015 presence data, since no Sal forest was sampled that year and all *M.*

micrantha presence records were in riverine forests along the Narayani River (Fig. 3-2). In addition, due to sun-sensor geometry, sunlit slope vegetation usually has higher reflectance and higher GV values before shade normalization in MESMA. Since the GV fraction is positively related to *M. micrantha* presence, sunlit slope vegetation pixels with high GV values can be assigned with higher presence probabilities. Despite fair model results, the presence data may not be sufficiently representative for predicting sites with distinct environmental conditions in the study area.

3.4.2 Incorporating elevation

In MESMA-fraction-only Maxent models (e.g. GV-Shade-NPV and GV-Shade-Soil), GV and Shade make prominent contributions to *M. micrantha* mapping, producing fair or good mapping results for both training and test datasets (Fig. 3-5). Nevertheless, according to the jackknife analysis in Maxent, although GV and Shade fractions are fair or good indicators of understory *M. micrantha* distribution (with-only AUC around 0.8), the most powerful predictor is elevation (with-only AUC above 0.9; Fig. 3-7). All GV-Shade-DEM Maxent models generate excellent map accuracies (AUC around 0.95; Fig. 3-5. c, f & i), and the contributions of elevation dwarf that of GV or Shade (Fig. 3-8). Map results show that the general distribution pattern is similar to those from fraction-only models, with *M. micrantha* presence allocated to pixels close to the Narayani and Rapti Rivers (Fig. 3-9). However, higher-elevation pixels are mostly assigned with low presence probabilities. This observation is in agreement with local knowledge that most *M. micrantha* is detected in riverine mixed forests, while invasion is less common in higher-elevation Sal forests.

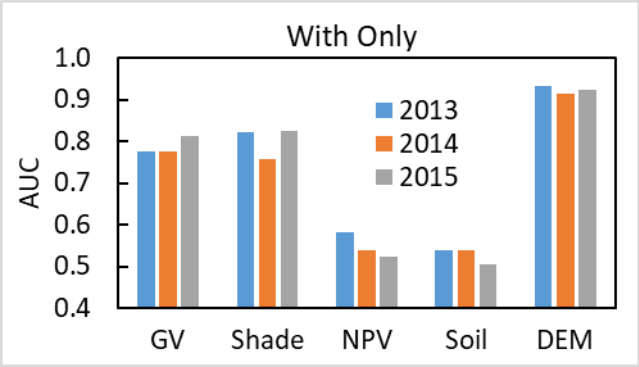

Figure 3-7: AUC values of Maxent models with only one of the predictors

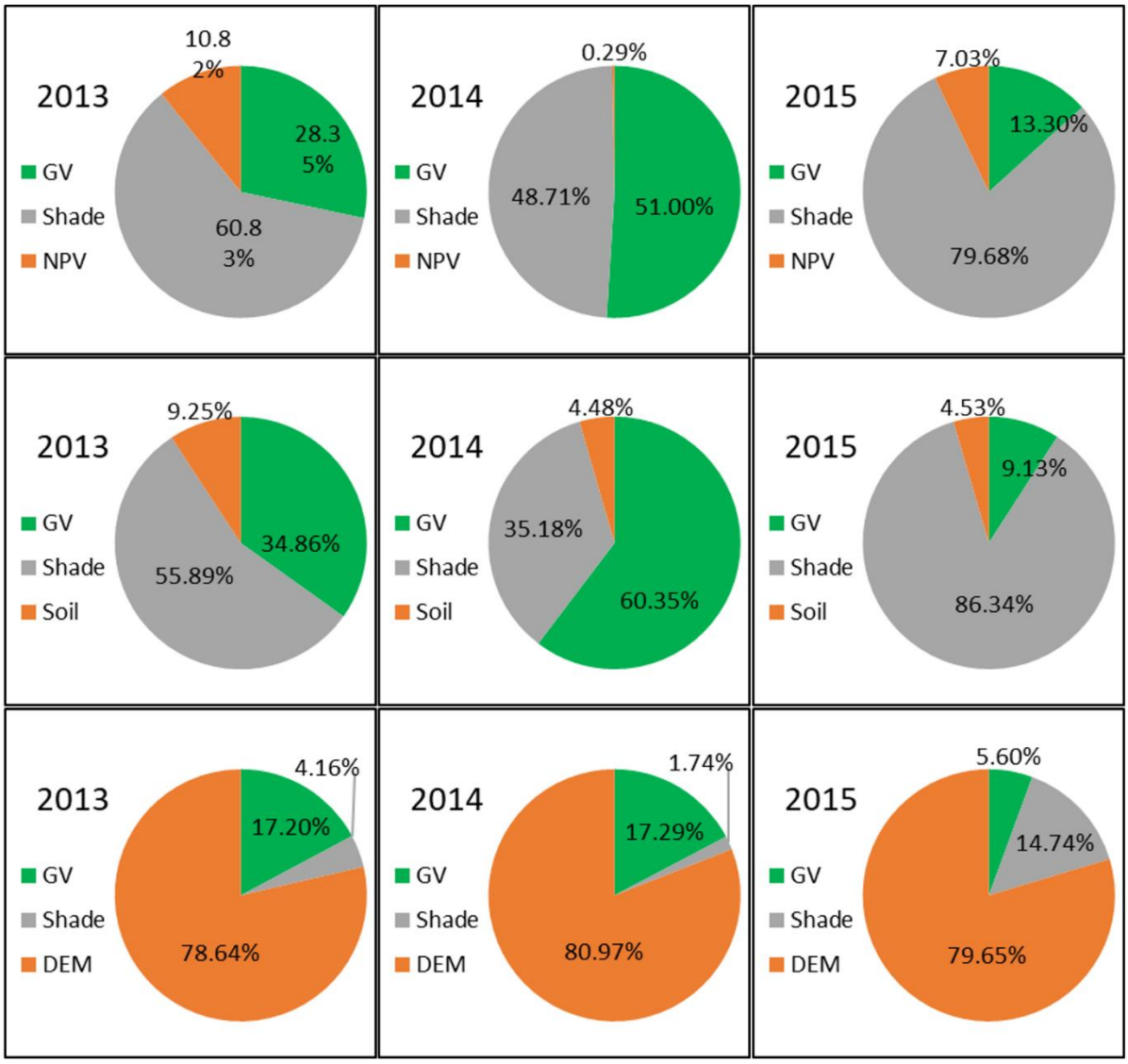

Figure 3-8: Predictors' contributions to their relevant Maxent models

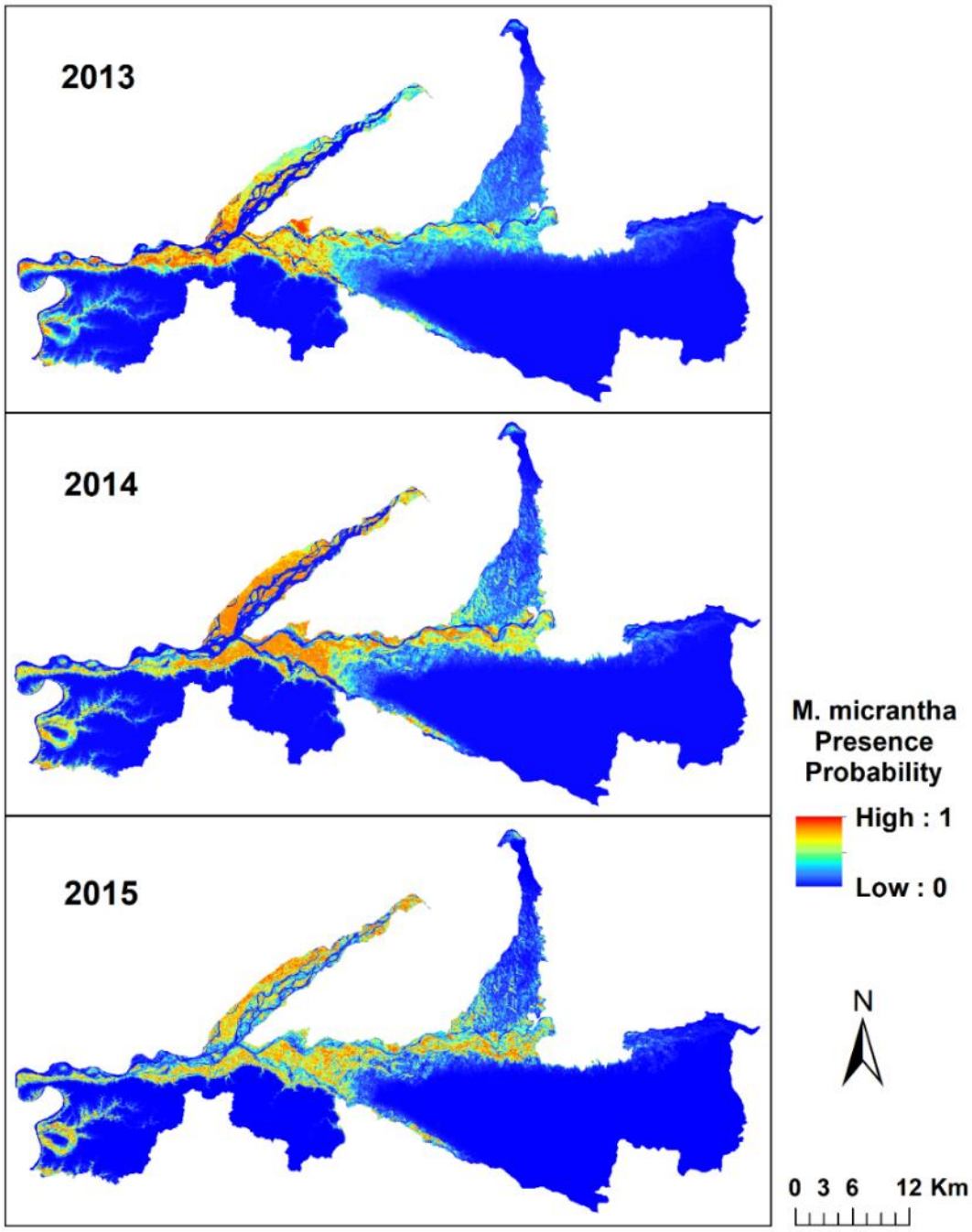

Figure 3-9: M. micrantha presence probability maps from GV-Shade-DEM Maxent models

Although elevation makes prominent contributions to the map results and it alone can generate excellent model outputs (With-only AUC above 0.9, Fig. 3-7), both MESMA fractions and elevation are critical in generating optimal *M. micrantha* distribution maps. Elevation alone may have produced good results for our training/testing dataset, which are the sample sites within the community forests, but it may not be sufficient for mapping the whole study area. If

elevation was the sole environmental layer, Maxent would assign high presence probabilities to all pixels with low elevation values, such as rivers and lakes (Fig. 3-10). Landscape factors like elevation may not be sufficient to explain ecological questions such as the distribution of certain species, thus biological factors should also be included. In this chapter, as indicators of forest structure and canopy conditions, the MESMA fractions are incorporated to produce optimal map results.

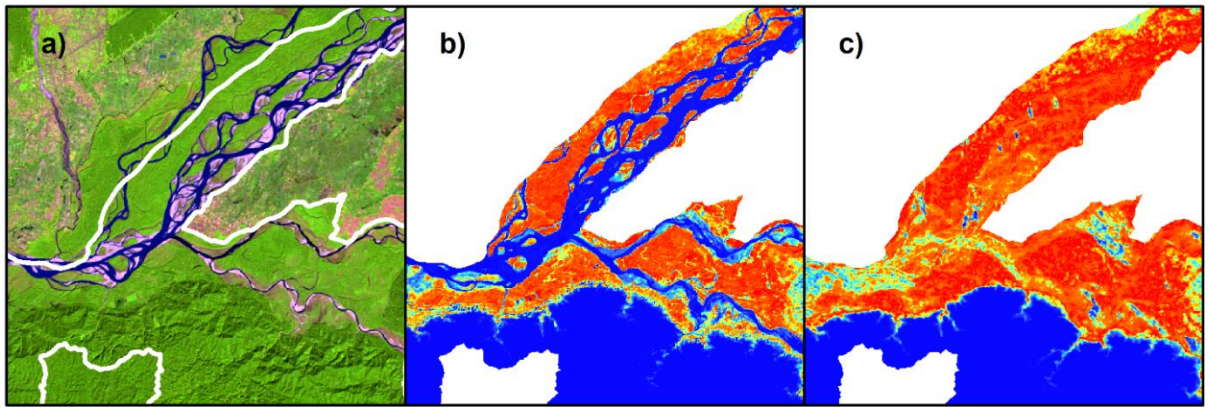

Figure 3-10: (a) depicts a subset of Fig. 3-1 where the Rapti River joins the Narayani River. Difference between GV-Shade-DEM (b) and DEM-only (c) Maxent models show that DEM-only models assigned high presence probabilities to non-vegetated pixels, including rivers and lakes.

3.4.3 *M. micrantha* invasion in Chitwan

Invasion ecology proposes that there are three main steps in the spread of an invasive species: first, an individual or a small population is transported from its native habitat to a geographically distant location it would otherwise not have reached through natural dispersal; secondly, this individual or population survives and reproduces in the new environment and forms sustainable communities; third, the exotic species thrives in the new environment and expands to its immediate neighbors or to more distant areas with the help of environmental or anthropogenic factors such as natural disasters and the movement of animals or humans (Lockwood et al., 2013). *M. micrantha* was introduced from the tropical and subtropical

Americas to India in World War II as camouflage for military facilities (Tiwari et al., 2005). It was first reported in eastern Nepal in the early 1960s and reached Chitwan in the early 1990s through catastrophic flooding according to local knowledge. *M. micrantha* is a fast-growing climber which can reproduce through sexual (seeds) or asexual (stems) processes, and its seeds are adapted to fire (Murphy et al., 2013). The stems and seeds of *M. micrantha* would first arrive at and inhabit riverine and riparian environments. After establishing sustainable populations and communities, it would invade higher-elevation habitats that are further away from rivers. In this case, proximity to a river would be the determining factor of the first wave of M. micrantha invasion. Besides, *M. micrantha* prefers and grows best in high soil moisture conditions (Zhang & Wen 2009). It is more likely to invade and thrive in low-lying areas having higher soil moisture. Our results show that by the year 2015, *M. micrantha* invasion in Chitwan National Park and its buffer zone community forests had mostly occurred in riverine forests and riparian grasslands.

3.4.4 Combination of MESMA and Maxent

In addition to the good agreement between the presence records and the *M. micrantha* distribution maps generated in this chapter, the method of combining MESMA and Maxent species distribution modeling provides a novel approach for mapping understory vegetation. In situations where direct detection with satellite data is obscured by canopy tops, Maxent modeling enables understory mapping through indirect methods. Compared to other indirect detection approaches which require additional temporal information through time series analysis of vegetation phenology, this approach only need the process of a single-time image (Tuanmu et al., 2010). Other than the presence records, the only other data needed are remotely

sensed which are open source and can be acquired conveniently from online sources. Besides, this approach can be easily extended to other understory plant species, as long as they introduce composition (e.g. GV and Shade fractions) changes alongside their growth.

3.5 Conclusions

It can be challenging to identify and map understory invasive plants through traditional remote sensing techniques due to the obstruction by canopies. In this chapter an effective and practical approach is developed to map understory invasive plant using endmember fractions derived from Landsat 8 OLI imagery and the Maxent modeling framework. The easy access, global coverage and rich historical archive of Landsat data make this approach applicable to a wide range of different study sites. It can also be applied to other satellite imagery with moderate/coarse spatial resolution and global coverage, such as Sentinel 2 data. The combination of MESMA and Maxent provides a significant opportunity for understanding understory vegetation distribution, not only about invasive non-native species, but also native shrubs and herbaceous species. The map results can provide guidance to local invasive plant eradication practices and conservation plans, substantially contributing to ecological restoration, biodiversity conservation, and provision of sustainable ecosystem services in protected areas.

4. Chapter IV: Invasive *Mikania micrantha* Control in Western Chitwan Community Forests, Nepal: An Agent-based Modeling Approach

4.1. Introduction

Mikania micrantha is a notorious creeping vine originated in the tropical Central and South Americas, and it has been invading the Chitwan National Park and its buffer zone community forests in Nepal since the late 1990s (Murphy et al. 2013). Due to its fast growth and unsuitable for herbivory, *M. micrantha* is disrupting forest ecosystems and biodiversity hotspots by hindering native vegetation growth, which is significant to the survival of endemic endangered species, such as the great one-horned rhinos and Bengal tigers (Dai et al., 2020; Murphy et al., 2013). The invasion of *M. micrantha* may also jeopardize the livelihoods of local residents by affecting the productivity of the community forests, upon which most of households rely directly or indirectly in varying degrees.

According to conversations and household surveys with local residents (described later), forest users have conducted jungle cleaning treatments in the past aiming to control the spread of *M. micrantha*. Common practice was to remove all herbaceous and woody vegetation except trees, collect them into a pile and burn *in situ*. This treatment method may promote invasion since *M. micrantha*'s seeds are adapted to fire and burning can eliminate competitors for natural resources (Murphy et al. 2013). To combat the spread of the invasive species, an ecological intervention with modified treatment practices has been designed, in which only invasive plants (including *M. micrantha*) are removed from the forests, and they are bagged and buried in one-meter-deep holes dug in the forest (Clark 2020).

The objective of this chapter is to simulate local household participation in the intervention,

and the subsequent responses of *M. micrantha* under modified intervention practices. The CNH research team ("the team" hereafter) conducted household surveys to collect a suite of socio-economic and demographic information which may affect willingness of household members to participate (An et al., 2014). The team also drew on field experiments to quantify the growth of *M. micrantha* and cost of labor and time for the intervention (Clark 2020). This chapter features development of a spatially explicit agent-based model using NetLogo software to simulate different levels of household participation in the large-scale intervention of the community forests, as well as how *M. micrantha*'s extent and coverage will respond to the intervention. The results provide significant insights in guiding local invasive plant intervention practices, conservation of ecosystems or ecosystem services, and more importantly, understanding impacts of human decisions on coupled human and natural systems.

4.2 Methodology

4.2.1 Study site

The study area of this chapter consists of the 21 community forests in the Chitwan National Park buffer zone and their catchment area households (Fig. 4-1). This study also includes a portion of the Chitwan National Park that is adjacent to the community forests, where intervention practices will not likely be conducted due to accessibility and the presence of dangerous animals. Nevertheless, *M. micrantha* may spread from these regions to cleaned community forests.

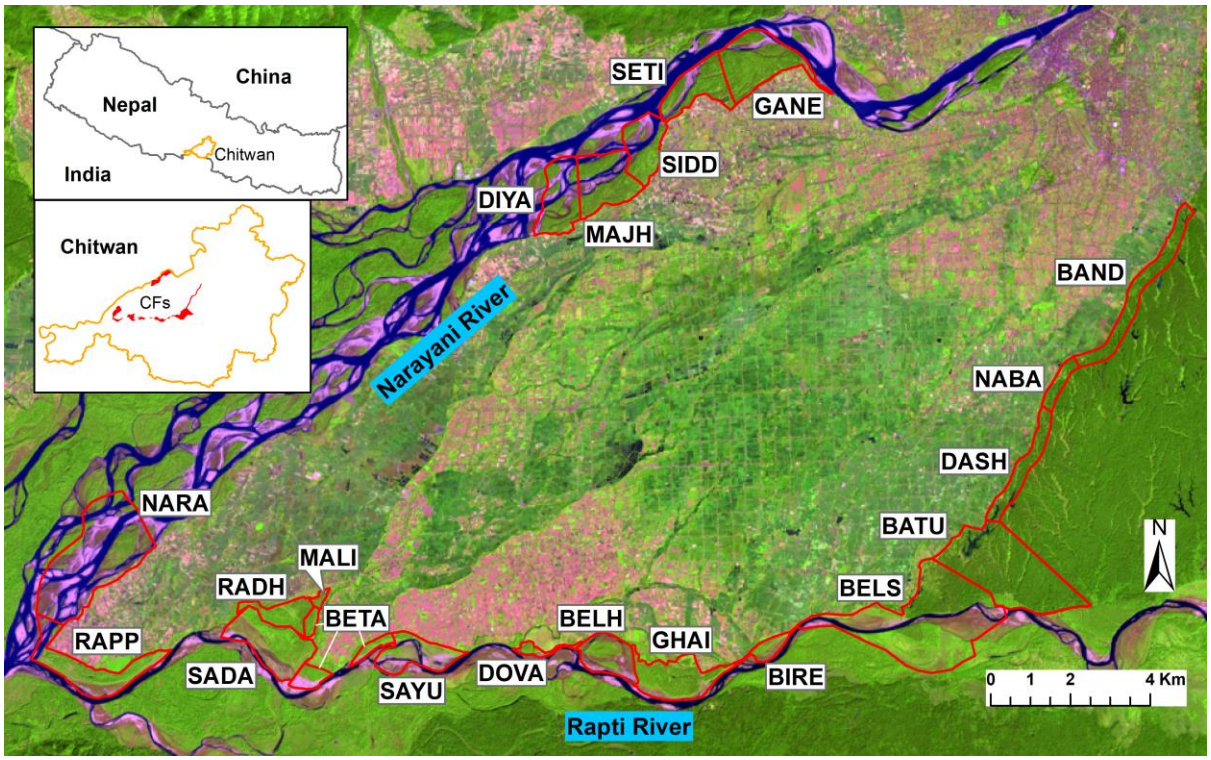

Figure 4-1: Image map of the community forests in the Chitwan study area

4.2.2 Social survey

The social survey team administered the first wave of household surveys in 2014. Through a systematic sampling scheme, around 50 households were selected from the catchment area of each community forest, as well as about 200 non-catchment households. The response rate was 98.6% and 1235 households were interviewed. The survey focused on 1) demographic information: household size, and the age, gender, education level of interviewed individuals; 2) household-level characteristics such as income sources, farming practices, land area, livestock raising and resource collection behavior; 3) household relationships to community forestry: membership of community forests, participation in forest committee and related user groups; 4) opinions on invasive species: the spread of *Mikania micrantha* and its effects on forest ecosystems, and 5) geographical information: longitude and latitude of each household.

In 2017, all households in the first wave survey were resurveyed with identical questions

and some new households that moved into the study area since 2014 were also included. Households that had moved out were tracked as well. This resulted in 1489 households being interviewed in the second wave of survey. In addition to all previous questions, households were also questioned about their willingness to participate in future large-scale *M. micrantha* intervention practices.

4.2.3 Field experiments

An ecological intervention was designed to test the feasibility of implementing a low-cost, effective, and sustainable set of practices to reduce the rate of spread of *M. micrantha* in the study area (Clark 2020). In November 2015, five community forests were selected to participate in the intervention (e.g. BELS, RADH, RAPT, SAYU, and DIYA; Figure 1). A total of 20 experiment plots were established with four in each forest. Each plot is 30 m by 30 m in area with a buffer of 5 m on each side, whereas all experimental and measurement activities were conducted within the core 20 m by 20 m area. The intervention involved multiple steps; several people conducted jungle cleaning and removed all invasive plants from their host plants or on the ground, meanwhile others dug holes in the forests. All removed *M. micrantha* was then bagged and buried deep in the holes. All experiments and measurements were conducted between November 2015 and October 2018. The experimental plots were set up in November 2015 and the first intervention took place in January 2016. Two additional intervention treatments were conducted in October 2016 and October 2017. For the intervention details please consult Clark (2020).

4.2.4 *M. micrantha* control model

In this chapter, the spatially explicit agent-based model integrated both ecological and

social factors to simulate household participation in *M. micrantha* intervention and the resulting *M. micrantha* presence probabilities in the community forests (Fig. 4-2). A social module simulated household participation in the intervention, while a cellular automaton-based ecological module was designed to examine *M. micrantha* responses to the intervention. For the ecological module, the model's start of simulation was set at 2015 (Time 0 in the model) and a *M. micrantha* coverage map of the same year was imported (Dai et al., 2020). For the social module, the simulation of household attribute dynamics was set to start in 2017 (Time 2). No prior interventions other than our field experiments had been conducted in the study area, so the large-scale *M. micrantha* intervention was set to be onset starting 2020 (Time 5). In the model there was no social impacts on the landscape before 2020, so that the ecological module could operate on its own without considering human impacts. The spatial resolution of the model was 30 m, identical to the *M. micrantha* presence map (Dai et al., 2020). The temporal resolution was one year, and the time span of simulation was 25 years (including 20 years of intervention starting in 2020).

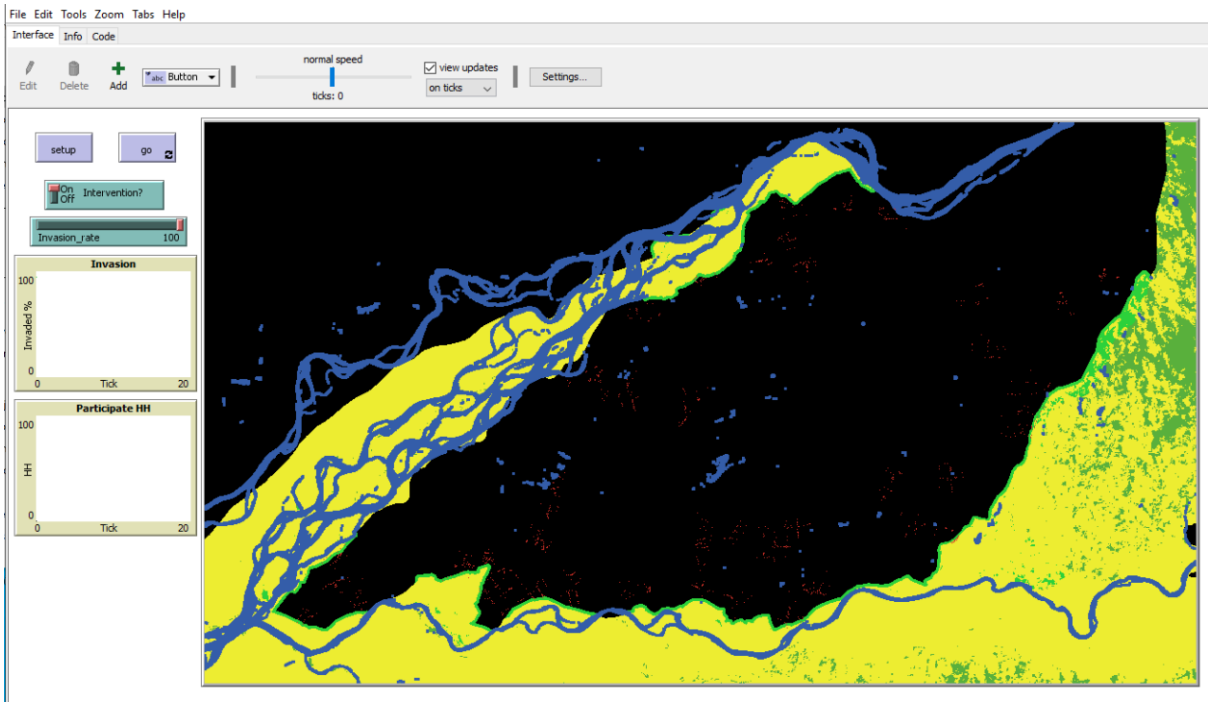

Figure 4-2: The interface of the model developed in NetLogo. The window on the right represents the community forests (lime), Chitwan National Park (green), water bodies (blue) and households (red; 1072 in total) against a black background depicting the landscape of the study area (1083 cells by 614 cells). Most of the forest and park cells are yellow and indicate *M. micrantha* invasion with varying degrees at the simulation start. The graphs on the left show the percentage of community forest cells being invaded and the number of households participating in intervention.

The agents in the model were the simulated households, who could decide on their participation in intervention based on a suite of social, demographic and geographic attributes. The environment consisted of landscape cells with attributes of being invaded by *M. micrantha* or not. In each time step, *M. micrantha* could spread in the study area, and then intervention could eradicate *M. micrantha* from the cells. The technical details of the model are presented in the following paragraphs, as well as in the Overview, Design concepts, & Details (ODD) appendix.

4.2.4.1 *M. micrantha* invasion

The *M. micrantha* presence probability map (Dai et al., 2020) was imported into the model as the initial state of *M. micrantha* prior to simulating its spread and removal. In the

cellular automaton based ecological module, once a cell was invaded by *M. micrantha*, it would have a probability of spread to any of its neighboring cells. This probability was flexible and controlled interactively by a slider in the model interface (Invasion_rate 0-100%; Figure 4-2). Given the notorious quick speed of grow and spread of *M. micrantha*, the invasion rate (probability) was set as 1.0 (e.g. 100%) in the baseline simulations. An important goal of this chapter is testing the model with different levels of invasion probabilities in a sensitivity analysis, described later in the model evaluation section.

4.2.4.2 Household decision in intervention participation

Based on previous pilot interviews and the 2017 household survey (1489 responding households), the team asked each household about their willingness to contribute at least ten full days of labor to *M. micrantha* intervention in the community forests each year. Here this chapter draws on a suite of socioeconomic, geographic, and demographic variables from the survey to quantify the households' probabilities of contribution and present our rationales.

About 54% of the households (806/1489) surveyed in the study area were general members of community forests, upon which their livelihoods relied in varying degrees. Some households directly extracted natural resources from the forests. For example, around 84% of the surveyed households (1253/1489) used firewood for cooking and other purposes, and 291 of them regularly collected firewood from the forests. About 63% of the surveyed households (935/1489) indicated that they raise cows, buffalos and/or goats, and 118 of them regularly collected fodder in the forests. Households may also be indirectly related to community forestry. About 74% of the households (1098/1489) were members of at least one user's group, such as women's group, forest user's group, saving and credit group, farmer's group, etc. (Baral et al.,

2019). These groups usually receive support from the community forests and their governance committees in the study area.

When examining households' motives in *M. micrantha* intervention in the community forests, a suite of potential factors that might affect their decisions were considered (Table 4-1). Since the invasion of *M. micrantha* jeopardizes forest productivity, households closely related to community forests might be willing to contribute to invasive plant removal. Independent variables thus included income sources (farming, business, and salary jobs), community forest membership, and participation in a user's group supported by community forestry. Because community forests are important sources of firewood and fodder, variables related to resource consumptions (use firewood or not, 1/0; number of livestock) were also included. According to local knowledge, a cow consumes about the same amount of fodder as a buffalo and about four times as much as a goat. Fodder consumption was thus represented by livestock amount, equal to four times the number of cows and buffalos plus the number of goats. Household geographic and demographic characters might also affect their decisions, and household distance to the community forests and household size (number of residents) were also included. The dependent variable was whether the household would be willing to contribute at least ten full days of labor for *M. micrantha* intervention each year (1 for yes and 0 for no). Generalized logistic regression was applied to analyze the relationships between the dependent and independent (listed in Table 4-1) variables.

Table 4-1: List of independent variables

Variables	Description	Mean	Min	Max	Std
HH_size	Number of residents	3.99	0	16	1.76
CF_dis	Household distance (kilometers) to community forest	1.37	0	4.80	1.15
CF_member	Community forest member or not (1/0)	0.54	0	1	0.50
User_group	User group member or not (1/0)	0.74	0	1	0.44
Farming	Income from farming or not (1/0)	0.76	0	1	0.43
Business	Income from business or not (1/0)	0.28	0	1	0.45
Salary	Income from salary jobs or not (1/0)	0.36	0	1	0.48
Firewood	Use firewood or not (1/0)	0.84	0	1	0.37
Livestock	Number of livestock	5.53	0	164	7.59

All independent variables were included in the logistic regression model and the results are presented in Table 4-2.

Table 4-2: Final variables included in the generalized logistic model

	Estimate	Std. Error	Z value	P value
(Intercept)	-1.197983	0.223301	-5.365	8.10E-08
CF_dis	-0.146668	0.052480	-2.795	5.19E-03
HH_size	0.065629	0.031928	2.056	3.98E-02
CF_member	0.125382	0.122034	1.027	0.30
Farming	0.199650	0.144517	1.381	0.17
Business	0.068230	0.124442	0.548	0.58
Salary	-0.046555	0.113728	-0.409	0.68
Livestock	-0.008416	0.008245	-1.021	0.31
Firewood	0.224656	0.169237	1.327	0.18
User_group	0.452033	0.131778	3.430	6.03E-04

Note: N = 1489; AIC: 1973.5; Pseudo R^2 =0.25

Incorporating the coefficients analyzed from the regression, the probability of household contributing at least ten full days of labor to *M. micrantha* intervention (Mik_prob) is:

Mik_prob = exp (-1.197983 – 0.146668 * CF_dis + 0.065629 * HH_size + 0.125382 * CF_member + 0.199650 * Farming + 0.068230 * Business – 0.046555 * Salary – 0.008416 * Livestock + 0.224656 * Firewood + 0.452033 * User_group) / (1 + exp (-1.197983 – 0.146668 * CF_dis + 0.065629 * HH_size + 0.125382 * CF_member + 0.199650 * Farming + 0.068230 * Business – 0.046555 * Salary – 0.008416 * Livestock + 0.224656 * Firewood + 0.452033 * User_group)) Equation (4.1)

During the modeling process, the potential changes in the demographic and social

characteristics above were informed by the two waves of household surveys. The 1235 households in 2014 with the 1489 households in 2017 were compared to locate those who were surveyed twice. A total of 1072 households were selected, upon which derived change patterns of household attributes, which would affect their intervention participation. Average household size, or the average number of residents who regularly lived in the household, was 4.143 and 4.118 in 2014 and 2017, respectively. The average change from 2014 to 2017 is -0.025 with most of the households' sizes remaining unchanged. Average livestock amount decreased by 0.994 between the two waves of surveys, from 7.444 in 2014 to 6.450 in 2017.

Among households who used firewood in 2014, 7.44% of them switched from using firewood to not using it in 2017, whereas 56.04% of the households who did not used firewood in 2014 switched to using firewood in 2017 (Table 4-3). Similar change patterns for other binary household attributes are listed in Table 4-3.

Table 4-3: The probabilities of changing binary household attributes from 2014 to 2017 based on surveys of 1072 households. 1 stands for positive responses, and 0 for negative ones.

	2014 (1) -> 2017 (0)	2014 (0) -> 2017 (1)
Firewood	0.0744	0.5604
User group	0.2513	0.8225
CF member	0.1722	0.3213
Farming	0.0922	0.3005
Business	0.3115	0.1613
Salary jobs	0.3166	0.2483

To simulate household participation in the intervention, the model first populated the 1072 households in the landscape based on their geographical information (longitude and latitude). Also, annual household attribute changes were modeled starting in 2018 (Time 3 in our simulation time span) to simulate household participation dynamics. The distances to forests were kept constant since they rarely changed between the two waves of survey. Since the

average change of household size was minimal (-0.025) and with most households unchanged, household size was also set to be constant for the simulations. For livestock amount, starting in Time 3 (year 2018), the value in the current step was set to be its value in the previous step minus a Poisson-distributed random integer with a mean of 0.994/3. If the new value was negative, it was set to zero. For all binary attributes, their change probabilities were informed by Table 4-3 and we divided them by three to account for annual changes. If the values did not change, they were kept the values in the previous step. Utilizing Equation (4.1), the household's probability of contribution in *M. micrantha* intervention were calculated. In the modeling process, if a randomly generated number between 0 and 1 was less than this probability, the corresponding household would contribute ten days of labor to the intervention.

Given the ratio of simulated households to the total number of households within all community forest catchment areas (1072/29418), the participation numbers were linearly upscaled to account for total available labor in the large-scale intervention. This decision was made for both theoretical and practical reasons (Zvoleff & An, 2014). First, the agents in our model were survey-based and are drawn from the population with a systematic sampling scheme, thus they were considered as representative of all households in the study area. Second, based on questions under hypothetical situations in the 2017 survey, some households would be affected if 75% or more of their neighbors participated in the intervention, whereas most of the households' decisions remained unchanged despite potential neighborhood impacts. Given the participation rate (around 40%) in the current real-world situation (2017 survey), interactions with neighbors can hardly change their decisions on intervention participation. Last, a practical concern was that modeling all of the 29148 households would significantly

slow down the simulations with little marginal benefits.

4.2.4.3 *M. micrantha* Intervention

In the field experiments, seven people could clean a 20 m by 20 m plot in 90 to 210 minutes (Clark 2020). The model set the intervention time to be a randomly selected number from a normal distribution between 90 min and 210 min, with a mean of 150 min and standard deviation of 30 min. Later in the sensitivity analysis (Section 4.2.4.4 an important test regarding the impact of different levels of fixed intervention times is featured.

To establish intervention locations, the model calculated the distances from each cell to the households. During intervention, cells closer to the households were cleaned first. Worthy of mention is that the participation rate was linearly upscaled to the whole population in the study area, which would also upscale the number of cells being cleaned in the intervention. However, this decision did not affect the locations of selected cells, since their selections were always based upon their distances to the households. Once a cell was cleaned, it could not be marked as "invaded" (invaded? = false) toward the end of current step. Based on the invasion rules articulated in Section 4.2.4.1, it might be re-invaded in future steps if one of its neighbors was invaded.

4.2.4.4 Model evaluation

The evaluation of the simulation processes consists of both model verification and validation (Manson 2002). Model verification guarantees that the programming code is free of bugs and fulfils the simulation objectives, whereas model validation compares model processes and results with expected ones from empirical data, real world observations, domain knowledge, or expert's opinions (An et al., 2005; An et al., 2020; Manson 2002).

The dynamics of simulated livestock amount of the households were examined for 20 years and the mean and standard deviation are compared to the data informed by the 2017 household survey. The dynamics of participating households were also examined for 20 years. As empirical data for the number of livestock amount and participating households after 2017 were unavailable, the simulation results from 2020 (start of household participation simulation) onward were compared to the participation ratio informed by the 2017 survey.

M. micrantha dynamics (percentage of forest cells being invaded and their locations) in response to the intervention were also validated in the community forests. Since the model projected future scenarios based on principles learned from empirical data but in totally different situations (intervention), it was examined based on whether change trends were reasonable.

Last, sensitivity analysis was performed through a parameter-sweeping approach (An et al., 2005; An et al., 2020). In Sections 4.2.4.1 through 4.2.4.3, the model performance might be sensitive to three parameters, i.e., *M. micrantha* invasion rate in the field, number of days each household contributed per year, and the intervention time cost. A sensitivity test was designed based on these three parameters: invasion rate was set at 0.2, 0.5, 0.8, and 1.0; number of contributing days of each household could be 2, 5, and 10; and the time needed to clean a 20 m by 20 m plot was be fixed at 90 min, 150 min, and 210 min. As there were four, three and three values for each parameter to test, respectively, there were a total of 4*3*3 = 36 experiments. The baseline scenario was set with 1.0 invasion rate-10 days participation -150 min clean-up combination since it was the closest to real-world situations. For each experiment, 30 model runs were conducted and *M. micrantha* extent maps were generated at the end of

simulation. Then the kappa index was calculated between each experiment map and the baseline map.

Model evaluation results will be discussed alongside presentation of simulation results, as well as in detail in Section 4.3.3.

4.3 Experiment design and simulation results

In the NetLogo model, the community forest landscape was comprised of 45138 non-water cells, 94.77% of which (42777 cells) were marked as "invaded" with varying *M. micrantha* coverage in the initial phase (Fig. 4-2). There were 29418 households in the study area, and in the 2017 survey, 39.56% (589/1489) of the households were positive about their intervention participation. Based on this background, the experiment designs and the simulation results are presented in the following paragraphs.

4.3.1 Households participation in intervention

The model first simulated the dynamics of several key household characteristics and examined the resulting household participations. These simulations were separated from the ecological module, and only household attributes calibrated in Section 4.2.4.2 would affect the simulation results. Starting from 2020 (Time 5 in the model), household intervention participation probabilities were calculated according to Equation (4.1), and the resultant numbers of participating households were modeled for 20 years. Thirty model runs were conducted to account for the stochastic processes included in the model, which might generate outliers or unexpected results.

Despite fluctuations, the numbers of participating households remained relatively stable over the 20 years of simulation (Fig. 4-3). On average, 428 out of the 1072 households

contributed to the large-scale *M. micrantha* intervention in the community forests each year. The participation rate was about 39.93%, close to the rate informed by the 2017 household survey (39.56%). Given the consistency among different model runs and the similar rate compared to actual participation rates, this modeling result was considered reasonable for the simulation objectives.

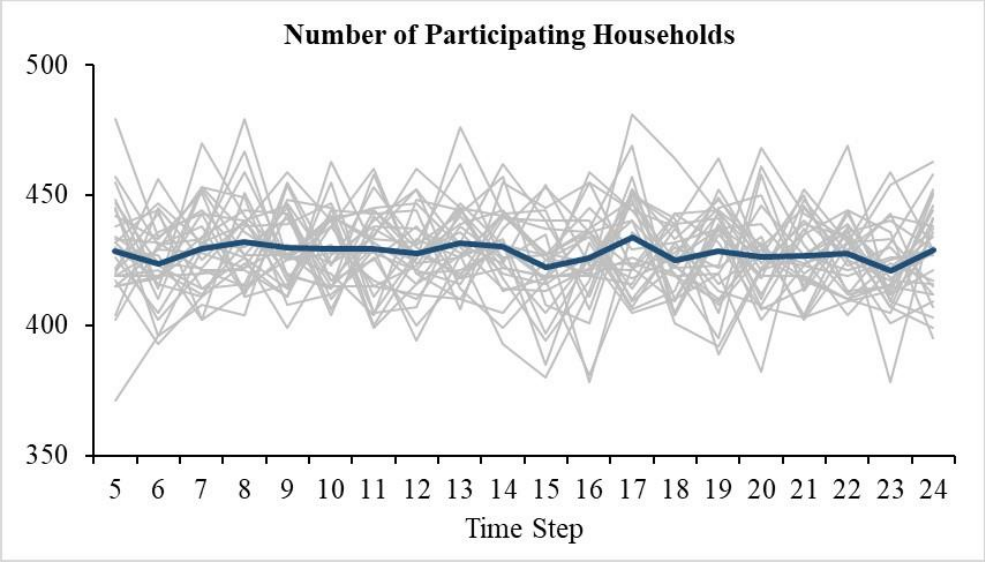

Figure 4-3: Number of participating households (30-run composite in gray) over 20 years with average number of each year highlighted in blue.

4.3.2 *M. micrantha* responses to intervention

The model then simulated *M. micrantha* responses to the intervention with inputs from the social module (Figures 4-4 & 4-5). In the simulation start (Time 0, Year 2015), 94.77% of the forest cells were invaded by *M. micrantha* (based on Dai et al., 2020), and the invasion extent gradually increased to almost 100% in Time 4 (Year 2019). After intervention starts in Time 5, the extents quickly dropped, and by the end of Time 7 (Year 2022), after three years of treatments, *M. micrantha* was completely eradicated from the forests (Extent = 0%). Note that this model did not simulate *M. micrantha* coverage in the cell, thus even 1% coverage would

be considered as “invaded”.

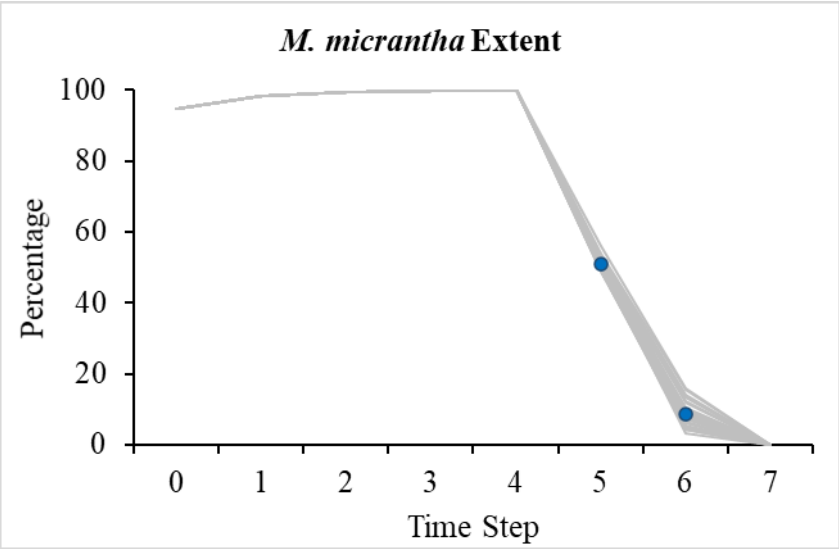

Figure 4-4: Percentage of forest cells being invaded by *M. micrantha* (30-run composite in gray) with average of the 30 runs in time steps five and six highlighted.

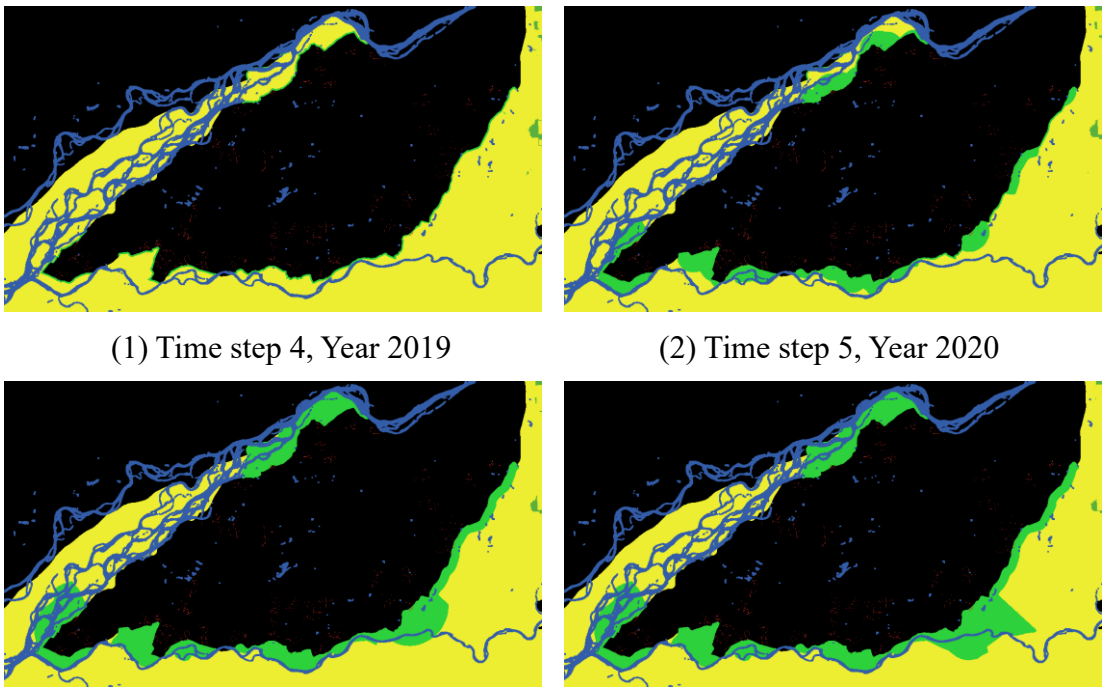

(1) Time step 4, Year 2019 (2) Time step 5, Year 2020

(3) Time step 6, Year 2021 (4) Time step 7, Year 2022

Figure 4-5: Average *M. micrantha* extent with invaded cells in yellow and cleaned cells in green at the end of time steps four to seven.

The simulated spatial locations of *M. micrantha* are shown in Fig. 4-5. Distribution patterns were similar among the 30 model-runs, and average outputs were presented for time

steps four to seven, corresponding to years 2019 to 2022. From simulation start (Time 0, year 2015) to Time 4 (year 2019), the spread and growth of *M. micrantha* was not affected by the output from the social module, and by the end of Time 4, almost all forest cells were invaded (Fig. 4-5 (1)). With the onset of the intervention treatments in Time 5, *M. micrantha* started being rapidly removed (Fig. 4-5 (2)). By the end of Time 7, the invasive plant was eliminated from the community forests, of which the map shows drastic comparisons with the outside national park, where intervention was not practiced (Fig. 4-5 (4)).

In addition to qualitative visual effects, several quantitative metrics were calculated to compare the differences between Times 5 and 7, as well as between Times 6 and 7 results. For each model run, the *M. micrantha* locations in the community forests at the end of Time 5 and Time 7 were compared, and each comparison generated a Kappa index (An et al., 2020; Cohen 1960). Then the Kappa indices from the 30 runs were averaged. The resultant averaging Kappa is 0.332. The processes were repeated between Times 6 and 7, and the averaging Kappa was 0.903, with the higher Kappa index indicating more similarity with the simulation end (*M. micrantha* completely removed from the community forests). Based on this change trend and the extend maps, the intervention resulted patterns where landscape cells closer to the households were prioritized in the intervention treatments, in consistent with the model design.

4.3.3 Model evaluation results

As discussed in Sections 4.3.1 and 4.3.2, the simulation results of household participation were mostly consistent among the 30 model-runs (Fig. 4-3), and the participation rate was similar to that informed by the 2017 household survey. As for *M. micrantha* extent, the results were also largely consistent among the 30 model runs (Figures 4-4 & 4-5). Its change trends

also make sense and reflect the simulation intentions.

Household livestock amount dynamics were also examined as described in Section 4.3.1 (Fig. 4-6). The average and standard deviation were close to the numbers informed by the 2017 household survey (6.28 and 7.08, respectively).

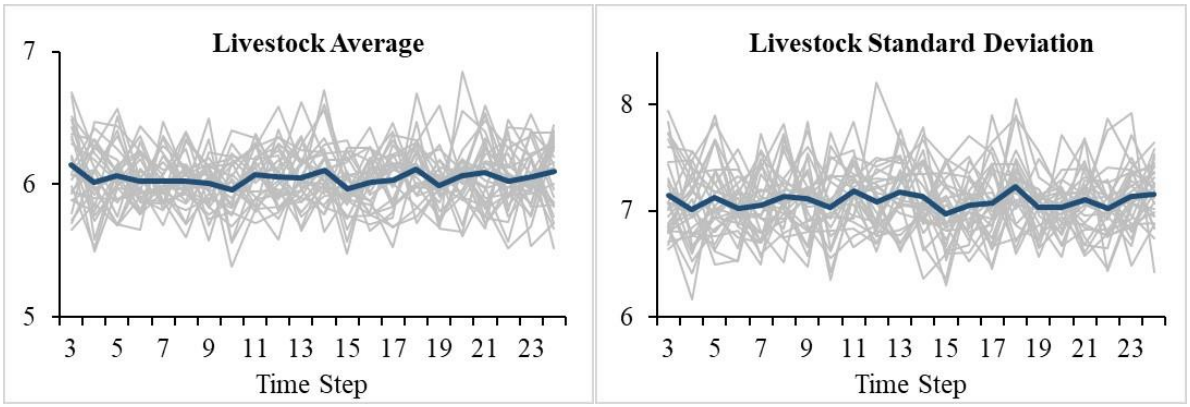

Figure 4-6: Average livestock amount of all model households and the standard deviation during the household intervention participation simulation described in Section 4.3.1.

The sensitivity analysis was conducted in two parts. In the first part, for each of the 36 scenarios mentioned in Section 4.2.4.4, the simulation continued until *M. micrantha* was completely removed from the community forests. Then the model reported the number of year's intervention needed to the simulation end (Table 4-4). The results varied dramatically among the different scenarios. In the baseline scenario (1.0-10 days-150 min), it took three years to completely eradicate *M. micrantha* from the community forest. When household contribution was high (10 days per year) and intervention time cost was low (90 min), *M. micrantha* could be eliminated after only two years of intervention. However, if household contribution was low (2 days per year) and intervention time cost was high (210 min), it might take 20 to 30 years to achieve the same goal. Comparing among the three parameters, the effect of invasion rate on the simulation results was less influential than household contribution and

intervention time cost in the tested ranges.

Table 4-4: Time span (number of years) needed for intervention to eliminate *M. micrantha* from the community forests under different scenarios. Low, moderate, and high contribution refers to participating households contributing 2, 5 and 10 days of labor each year, respectively. Low, moderate, and high intervention time cost refers to it takes seven people to clean a 20 m by 20 m plot in 90 min, 150 min, and 210 min, respectively.

		Intervention time cost		
Invasion Rate	Contribution	Low	Moderate	High
1.0	Low	8	17	32
	Moderate	3	5	8
	High	2	3*	4
0.8	Low	8	16	29
	Moderate	3	5	7
	High	2	3	4
0.5	Low	8	14	24
	Moderate	3	5	7
	High	2	3	4
0.2	Low	7	12	19
	Moderate	3	5	7
	High	2	3	3

* Baseline scenario

In the second part of sensitivity analysis, based on the intervention years informed by the baseline scenario, the model allowed the intervention simulation to run for three years and the resultant *M. micrantha* extents between the baseline scenario and the other 35 scenarios were compared (Table 4-5). Thirty runs were made for each scenario. For Scenario 1 (S1: 1.0-low-low) in Table 4-4, Run 1 was compared with Run 1 of the baseline setting, and the Kappa was calculated for Run 1, and was repeated for Run 2, Run 3, … up to Run 30. Then an average Kappa was calculated for S1 from the 30 Runs. And this process was replicated for all non-baseline scenarios. Their average Kappa values were reported in Table 4-5. In the simulations for different scenarios, if *M. micrantha* could be eliminated from the forests after three years (or less) of intervention, the Kappa for that scenario would be 1, since the simulation end

indicates the same result: *M. micrantha* being completely removed (Fig. 4-7). The lower Kappa values indicate lower similarities with the baseline scenario, and therefore more *M. micrantha* was present in the forests after three years of intervention.

Table 4-5: Average Kappa of 30 model runs after three years of intervention when comparing each scenario with the baseline scenario. Low, moderate, and high contribution refers to each household contributing 2, 5 and 10 days of labor each year, respectively. Low, moderate, and high intervention time cost refers to it takes seven people to clean a 20 m by 20 m plot in 90 min, 150 min, and 210 min, respectively.

		Intervention time cost		
Invasion Rate	Contribution	Low	Moderate	High
1.0	Low	0.2629	0.0916	0.0404
	Moderate	1.0000	0.5388	0.3037
	High	1.0000	*	0.9482
0.8	Low	0.2692	0.0943	0.0419
	Moderate	1.0000	0.5460	0.3038
	High	1.0000	1.0000	0.9563
0.5	Low	0.2709	0.0986	0.0454
	Moderate	1.0000	0.5561	0.3101
	High	1.0000	1.0000	0.9856
0.2	Low	0.3046	0.1150	0.0556
	Moderate	1.0000	0.6022	0.3493
	High	1.0000	1.0000	1.0000

* Baseline scenario

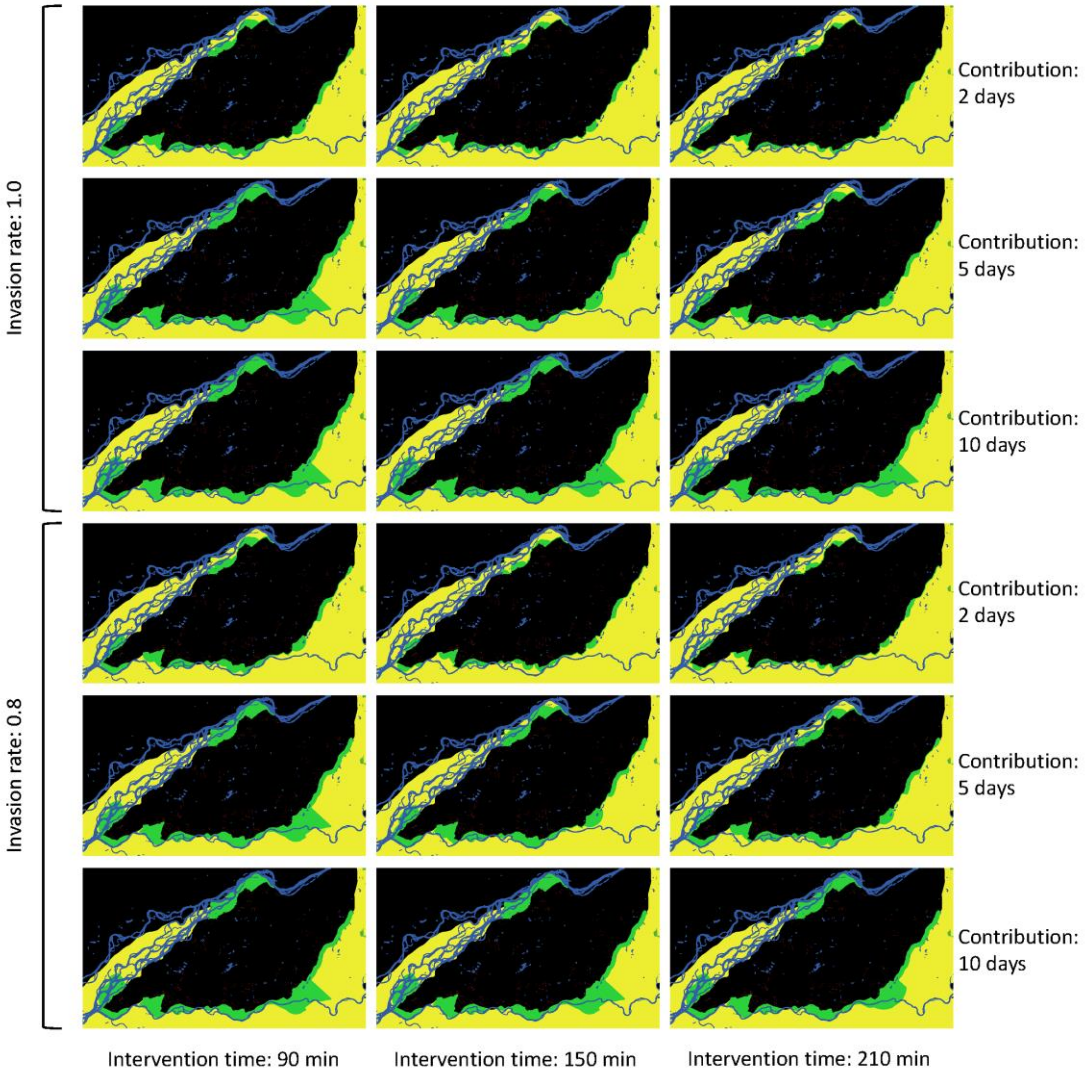
Invasion rate: 1.0
Invasion rate: 0.8
Contribution: 2 days
Contribution: 5 days
Contribution: 10 days
Contribution: 2 days
Contribution: 5 days
Contribution: 10 days
Intervention time: 90 min
Intervention time: 150 min
Intervention time: 210 min

(a)

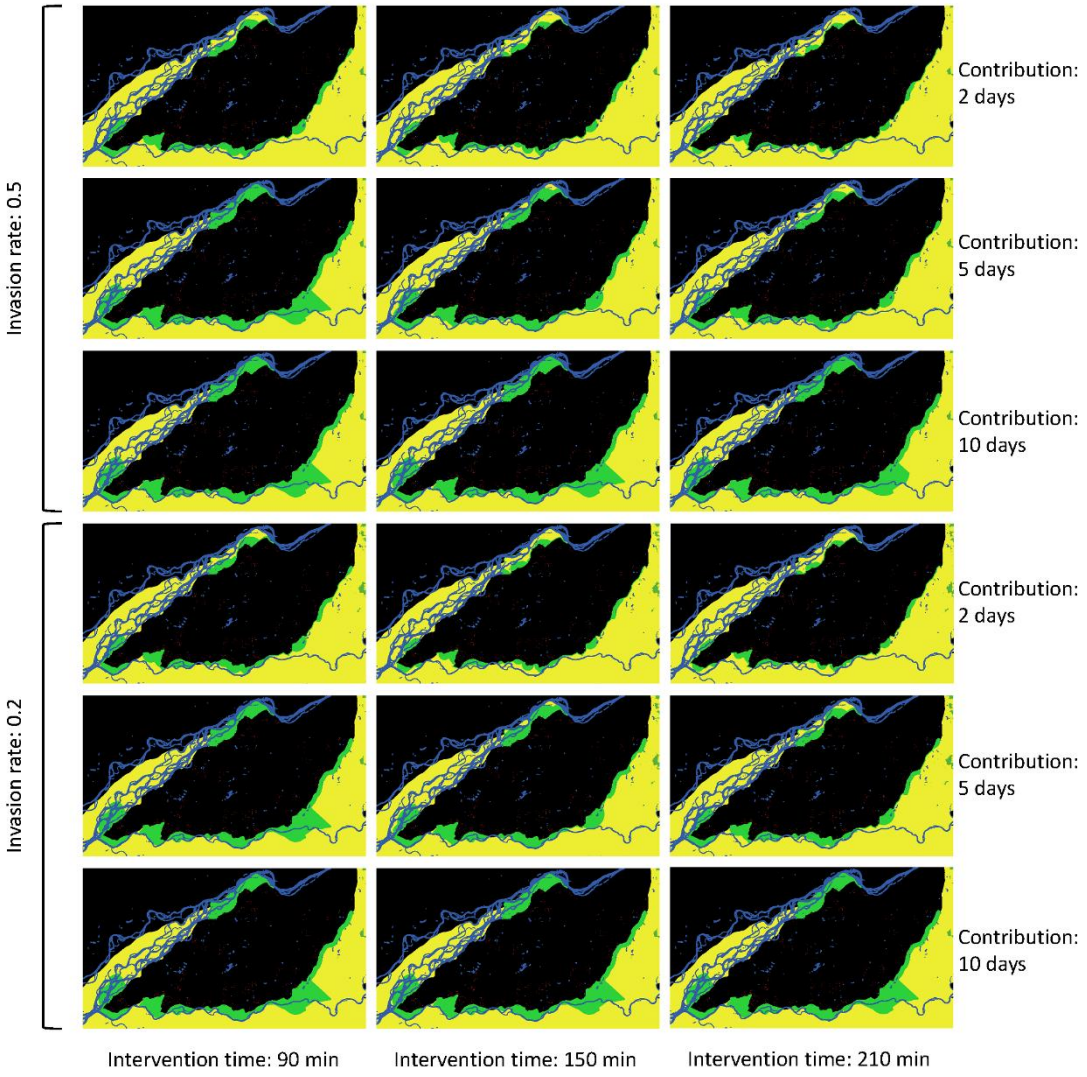

(b)

Figure 4-7: Average *M. micrantha* extent after three years of intervention under each of the 36 experiments. (a) presents the results for invasion rates of 1.0 and 0.8, whereas (b) is for invasion rates of 0.5 and 0.2. Intervention time stands for the time needed to clean a 20 m by 20 m plot. Green stand for cleaned (*M. micrantha* free) cells whereas yellow ones are invaded.

4.4 Discussion

In the model design, the priorities for cell cleaning are based on their distances to the households. Because all modeled households were surrounded by the community forests, this model setting creates a clustered pattern of intervention locations (Figures 4-5 & 4-7). To test the effects of this geographic attribute on intervention results, the model tests the baseline scenario (1.0 invasion rate - 10 days participation -150 min clean-up) but altering the settings

so that intervention locations were randomly picked from the forests. Again, the simulations were run for 30 times. The results are distinct from that with original model settings and after 20 years of intervention, *M. micrantha* invasion is still prominent in the forests (Fig. 4-8) with reminiscent invasion scattered in the forest landscape. These results may arise from the following processes: scattered intervention efforts will create much more invasion frontiers than clustered intervention, so that many more cleaned cells will be re-invaded in the next time step. This finding provides important insights that intervention treatments should be organized in a clustered manner, starting from one side of the forest and pushing toward the other side.

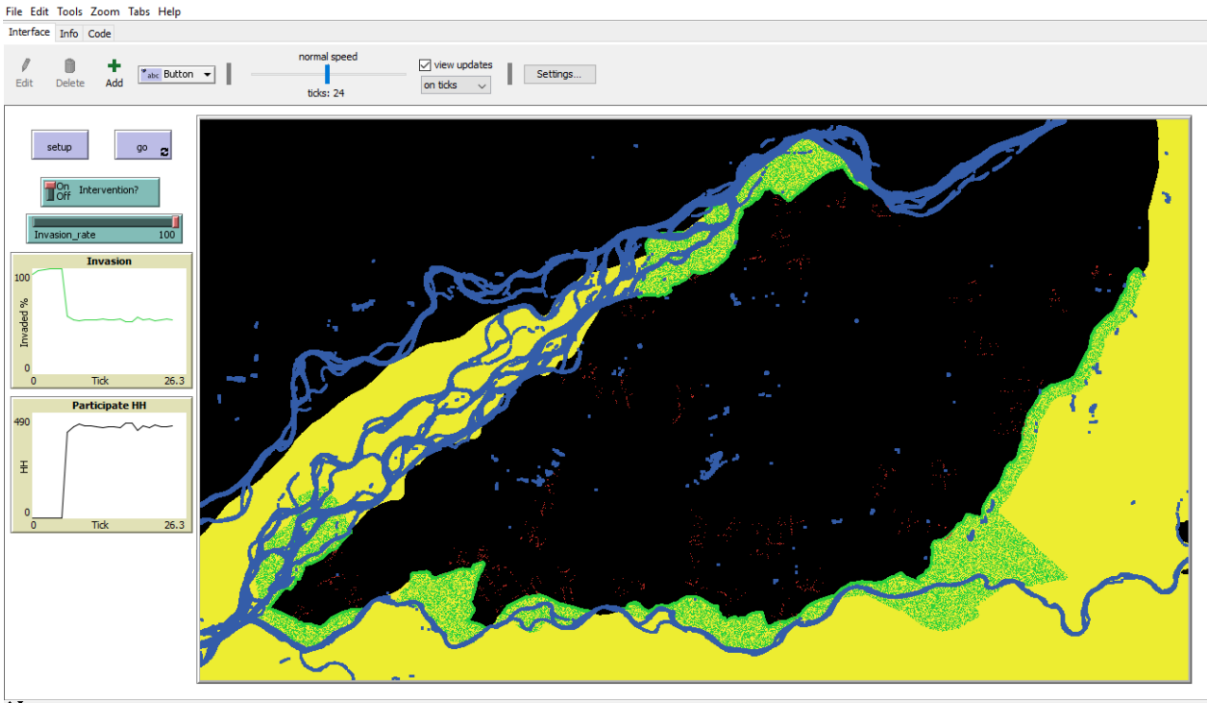

Figure 4-8: Simulation results if intervention locations were randomly selected.

It should be noted that household participation might have been underestimated in the above simulations. A cut-off threshold of ten days was designated for each household because it was the average number indicated in the pilot survey, and the number was also consulted with local experts to get their positive feedbacks. In practical situations, there may be cases

where participants can contribute more than ten days, and more than one member from the household is willing to participate in the intervention. There may also be households who cannot set aside ten full day due to various reasons, but can contribute less time, for example five days. In terms of implications for future large-scale intervention, if the goal is to eliminate the invasion within a certain designated region in short time, the more households contribute, the more quickly the objectives can be met. Community forest committees may organize the intervention in a flexible manner, so that each willing household can contribute certain days of labor toward the removal of *M. micrantha*.

Besides, the model only simulated *M. micrantha* eradication in the community forests, but not for the neighboring Chitwan National Park, where *M. micrantha* invasion was also pervasive (Dai et al., 2020). Ideally *M. micrantha* in both the community forests and the adjacent park area should be coherently removed, otherwise the park areas surrounding the community forests will continue to serve as sources of invasion. Nevertheless, intervention in the park can be risky due to potential encounters with dangerous animals, such as Bengal tigers and rhinos. If intervention in the park is impractical or limited, community forest users may need to routinely patrol and intervene in the forests neighboring the park (mostly along the Rapti River) for potential future invasions.

In summary, the merits of this chapter lie in the following aspects. First, this chapter is innovative in applying a coupled human and natural systems (CHANS) approach and incorporating socioeconomic factors in invasive plant control. Participants of the large-scale intervention campaigns are households and their members, who can make decisions and act in response to various socioeconomic characteristics. These attributes are calibrated from

household surveys and household's participation is quantified through regression analysis. In addition to the social factors, the responses of *M. micrantha* extent is also informed by a cellular automaton-based landscape module. All such processes take place on a spatially explicit landscape. In this context, the simulation is informed by knowledge from both natural and social disciplines and evaluates the dynamics of a socio-ecological system using an agent-based modeling approach.

Also, results from this chapter provide local forest users with important conservation and management insights. The most effective intervention practices are to enlist participation by as many households as possible and concentrate efforts in a clustered manner, instead of scattering treatments in different parts of the forests. It is also suggested that the organization of intervention should be flexible to include as many laborers as possible from forest users. Furthermore, the agent-based modeling practice contributes to model transparency and reusability (code available in the CoMSES) in the agent-based modeling domain.

Caveats may arise concerning intervention time in the field. In the agent-based model, the dynamics of *M. micrantha* coverage is simulated in the cells. Since the intervention involves clearing all invasive plants from the forests, not only *M. micrantha*, the amount of *M. micrantha* in a cell may have a positive effect on the intervention time cost. In the field experiments, the intervention time ranges from 90 min to 210 min, with varying *M. micrantha* coverage in the plots. Sensitivity analysis was thus designed to test different levels of intervention time costs.

Also worth mentioning is that the participation rate is linearly scaled up from modeled households to all households within the study area. As indicated by the 2017 survey, households may change their decisions in intervention participation if high percentage (e.g. 75% or above)

of their neighbors participated. Although in the simulations, as well as informed by the 2017 survey, the participation rates are much lower (e.g. 40%), there may be local neighborhoods where most households decide to contribute. In the future, experiments may be designed to test the impact of percentage of neighbors willing to participate in the program.

4.5 Conclusion

In this chapter, an agent-based model informed by socio-ecological data is developed and tested to project local household participation in *M. micrantha* intervention in Chitwan community forests, Nepal, as well as *M. micrantha*'s extent under the intervention practices. Based on modeled participation rates, if about 40% of the households in the study area contribute at least ten full days of labor to the modified intervention treatments, *M. micrantha* is projected to be eliminated from the community forests after three years, although routine patrolling should be adopted to eradicate potential future invasion from neighboring Chitwan National Park. It is recommended that the intervention should be carried out in a geographically clustered manner instead of diffusing efforts to all parts of the forests. The results provide significant insights for local users in terms of invasive plant control and sustainable community forests management. Broadly, this chapter also contributes to achieving the United Nation's Sustainable Development Goals (United Nations 2016), especially Goal 15 that aims to sustainably manage forests and halt biodiversity loss.

5. Chapter V: Conclusions

Through this dissertation research I examined the historical vegetation dynamics and the invasions of *Mikania micrantha* in western Chitwan community forests and how local communities can control the invasion. Inspired by the interdisciplinary coupled human and natural systems (CHANS) framework (Liu et al., 2007), this dissertation employs quantitative geospatial methods such as remote sensing to examine the historical greening-up signals of the targeting forests (Chapter II) and the spatial extent of *M. micrantha* invasion (Chapter III). This dissertation also features development of an agent-based model to simulate invasive plant intervention in the forests (Chapter IV). Below is a review of the major findings from each chapter.

Chapter II examines the green vegetation dynamics in the community forests for the past three decades, spanning from 1988 (before the 1993 Community Forestry Act) to 2018. Informed by the results generated from Multiple Endmember Spectral Mixture Analysis (MESMA) and the resultant Normalized Difference Fraction Index (NDFI), the western Chitwan community forests have been greening up since their establishments in the mid-1990s. Although the invasion of *M. micrantha* may have contributed to some of the detected signals, we can at least verify that community forestry management was the prime reason for reforestation in the inland Sal forests, where *M. micrantha* invasion was rare.

Chapter III integrates MESMA and Maximum Entropy (Maxent) modeling framework to map the presence probabilities of *M. micrantha* in the community forests. According to the modeling results, *M. micrantha* presence was positively related to the Green Vegetation fractions and negatively related to the Shade fractions produced by MESMA. Nevertheless, the

invasion was most sensitive to elevation, also a surrogate for distance to rivers, with invasion most prominent in riverine habitats. By the year of 2015, invasion was most prominent in the riverine forests and grasslands.

Chapter IV utilizes an agent-based model (ABM) to investigate household participation in a proposed large-scale invasive plant intervention campaign, and the response of *M. micrantha* to the intervention. Based on simulated participation rate of the households in the study area, as well as the designated contribution of labor, *M. micrantha* can be eliminated from the community forests after three years of intervention. The results suggest that concentrating the intervention locations in community forest areas instead of scattering efforts in different parts of the forests, in order to minimize potential frontiers of re-invasion. Recommendations from the work in this chapter are many. For instance, if the national park area adjacent to the forests are impractical to intervene, routine patrolling should be organized to clean any potential future invasions.

Broader Impacts and Future Directions

This dissertation addresses the "protection, restoration and promotion of sustainable use of terrestrial ecosystems", identified by the United Nations as one of the Sustainable Development Goals (United Nations 2016). Facing the novel challenges introduced by the invasion of exotic plant species, this dissertation mapped the spatial extent of the invasive plant and modeled its control in the western Chitwan community forests Furthermore, this dissertation may shed significant insights toward intervention practices, specifically contributing to the sustainable development goals.

Evaluating the functioning of forest ecosystems has long been the research focus of

sustainability science through both field inventory and remote detection techniques (Coppin and Bauer, 1996; Kim et al., 2014). Traditional remote sensing methods, especially direct detection, can readily assess forest top canopies, but researchers may have to be creative when novel challenges emerge. In this dissertation, the invasion of an understory creeping vine was mapped by integrating spectral mixture analysis (MESMA) and species distribution modeling (Maxent). Future research may incorporate active remote sensing techniques, such as Light Detection and Ranging (LiDAR) to better capture forest structure changes introduced by the invasion.

In addition to examining the potential responses of forests to environmental changes, novel tools, such as agent-based modeling (ABM), may be employed to simulate and project forest management outcomes under different scenarios (An et al., 2005; An et al., 2020). Particularly, in coupled human and natural systems (CHANS) where social and ecological factors may interact with each other, ABM can better capture the complex relationships among different modeling sectors (An et al., 2005; An et al., 2020; Liu et al., 2007). This dissertation has specifically contributed to the modeling of CHANS, as well as ABM testing, model transparency and reusability, and model of human decisions (An 2012). The CHANS and ABM approach offers a comprehensive framework for examining not only local conservation topics, but also broader sustainability related issues. Researchers from different disciplines may leverage this approach to better address complex socio-ecological questions.

6. References

Adams, J.B., Sabol, D.E., Kapos, V., Filho, R.A., Roberts, D.A., Smith, M.O. & Gillespie, A.R. (1995). Classification of multispectral images based on fractions of endmembers: Application to land-cover change in the Brazilian Amazon. *Remote Sensing of Environment*, 52, 137-154.

An, L. (2012). Modeling human decisions in coupled human and natural systems: Review of agent-based models. *Ecological Modelling*, 229, 25-36.

An, L., Linderman, M., Qi, J., Shortridge, A. & Liu, J. (2005). Exploring complexity in a human-environment system: An agent-based spatial model for multidisciplinary and multiscale integration. *Annals of the Association of American Geographers*, 95(1), 54-79.

An, L., Mak, J., Yang, S., Lewison, R., Stow, D.A., Chen, H.-L., Xu, W., Shi, L. & Tsai, Y.-H. (2020). Cascading impacts of payments for ecosystem services in complex human-environment systems. *Journal of Artificial Societies and Social Simulation*, 23(1), 5.

An, L., Zvoleff, A., Liu, J. & Axinn, W. (2014). Agent-based modeling in coupled human and natural systems (CHANS): Lessons from a comparative analysis. *Annals of the Association of American Geographers*, 104(4), 723-745.

Asner, G.P., Knapp, D.E., Kennedy-Bowdoin, T., Jones, M.O., Martin, R.E., Boardman, J. & Hughes, R.F. (2008). Invasive species detection in Hawaiian rainforests using airborne imaging spectroscopy and LiDAR. *Remote Sensing of Environment*, 112, 1942-1955.

Asner, G.P. & Vitousek, P.M. (2005). Remote analysis of biological invasion and biogeochemical change. Proceedings of the National Academy of Sciences, 102, 4383-4386.

Baldridge, A., Hook, S., Grove, C., & Rivera, G. (2009). The ASTER Spectral Library version 2.0. *Remote Sensing of Environment*, 113, 711-715.

Baral, S., Chhetri, B.B.K., Baral, H. & Vacik, H. (2019). Investments in different taxonomies of goods: What should Nepal's community forest user groups prioritize? *Forest Policy and Economics*, 100, 24-32.

Barbosa, J.M., Asner, G.P., Martin, R.E., Baldeck, C.A., Hughes, F., & Johnson, T. (2016). Determining subcanopy *Psidium cattleianum* invasion in Hawaiian forests using imaging spectroscopy. *Remote Sensing*, 8, 33.

Bradley, B.A. (2014). Remote detection for invasive plants: A review of spectral, textural and phenological approaches. *Biological Invasions*, 16, 1411-1425.

Bradley, B.A., Curtis, C.A., Fusco, E.J., Abatzoglou, J.T., Balch, J.K., Dadashi, S. & Tuanmu, M. (2018). Cheatgrass (Bromus tectorum) distribution in the intermountain Western USA and

its relationship to fire frequency, seasonality, and ignitions. *Biological Invasions*, 20, 1493-1506.

Carter, N.H., Shrestha, B.K., Karki, J.B., Pradhan, N.M.B. & Liu, J. (2012). Coexistence between wildlife and humans at fine spatial scales. *PNAS*, 109, 15360-15365.

Central Bureau of Statistics-Nepal. (2011). VDC Wise Population and Households Numbers. Retrieved from https://cbs.gov.np/ on December 30, 2019.

Charnley, S. & Poe, M.R. (2007). Community forestry in theory and practice: Where are we now? *Annual Review of Anthropology*, 36, 301-336.

Clark, M. (2020). *Evaluating the Social and Ecological Drivers of Invasive Plant Species Abundance in Sub-tropical Community Forests of Nepal (Doctoral Dissertation)*. Tempe, AZ: Arizona State University.

Cohen, J. (1960). A coefficient of agreement for nominal scales. *Educational and Psychological Measurement*, 20 (1), 37-46.

Coppin, P.R., Bauer, M.E. (1996).Digital change detection in forest ecosystems with remote sensing imagery. *Remote Sensing Reviews*, 13, 207-234.

Craig, R.K. (2010). "Stationarity is dead" – long live transformations: Five principles for climate change adaptation law. *Harvard Environmental Law Review* 34, 9-75.

Critical Ecosystem Partnership Fund (CEPF). (2020). Retrieved from http://www.cepf.net/resources/hotspots/Asia-Pacific/Pages/Himalaya.aspx.

Dennison, P.E., Halligan, K.Q. & Roberts, D.A. (2004). A comparison of error metrics and constraints for multiple endmember spectral mixture analysis and spectral angle mapper. *Remote Sensing of Environment*, 93, 359-367.

Dennison, P.E. & Roberts, D.A. (2003). Endmember selection for multiple endmember spectral mixture analysis using endmember average RMSE. *Remote Sensing of Environment*, 87, 123-135.

Dai, J., Roberts, D.A., Stow, D.A., An, L., Hall, S.J., Yabiku, S.T. & Kyriakidis, P.C. (2020). Mapping understory invasive plant species with field and remotely sensed data in Chitwan, Nepal. *Remote Sensing of Environment*, 250, 112037.

Dietze, M.C., Fox, A., Beck-Johnson, L.M., Betancourt, J.L., Hooten, M.B., Jarnevich, C.S., Keitt, T.H., Kenney, M.A., Laney, C.M., Larsen, L.G., Loescher, H.W., Lunch, C.K., Pijanowski, B.C., Randerson, J.T., Read, E.K., Tredennick, A.T., Vargas, R., Weathers, K.C. & White, E.P. (2018). Iterative near-term ecological forecasting: Needs, opportunities, and

challenges. *Proceedings of the National Academy of Sciences* 115, 1424-1432.

Ezeh, A.C., Bongaarts, J. & Mberu, B. (2012). Global population trends and policy options. *The Lancet*, 380, 14-20.

Feyisa, G.L., Meilby, H., Fensholt, R. & Proud, S.R. (2014). Automated Water Extraction Index: A new technique for surface water mapping using Landsat imagery. *Remote Sensing of Environment*, 140, 23-35.

Fielding, A.H. & Bell, J.F. (1997). A review of methods for the assessment of prediction errors in conservation presence/absence models. *Environmental Conservation*, 24, 38-49.

Gilmour, D. (2016). Forty years of community-based forestry: A review of its extent and effectiveness. Food and Agriculture Organization of the United Nations, Rome.

Grimm, V., Berger, U., Bastiansen, F., Eliassen, S., Ginot, V., Giske, J., Goss-Custard, J., Grand, T., Heinz, S. K., Huse, G., Huth, A., Jepsen, J. U., Jørgensen, C., Mooij, W. M., Müller, B., Pe'er, G., Piou, C., Railsback, S. F., Robbins, A. M., Robbins, M. M., Rossmanith, E., Rüger, N., Strand, E., Souissi, S., Stillman, R. A., Vabø, R., Visser, U. & DeAngelis, D. L. (2006). A standard protocol for describing individual-based and agent-based models. *Ecological Modelling*, 198(1-2), 115-126.

Grimm, V., Berger, U., DeAngelis, D. L., Polhill, J. G., Giske, J. & Railsback, S. F. (2010). The ODD protocol: A review and first update. *Ecological Modelling*, 221(23), 2760-2768.

Hoyos, L.E., Gavier-Pizarro, G.I., Kuemmerle, T., Bucher, E.H., Radeloff, V.C., & Tecco, P.A. (2010). Invasion of glossy privet (*Ligustrum lucidum*) and native forest loss in the Sierres Chicas of Cordoba, Argentina. *Biological Invasions*, 12, 3261-3275.

Huete, A.R. (1988). A Soil-Adjusted Vegetation Index (SAVI). *Remote Sensing of Environment*, 25, 295-309.

Huete, A.R. & Post, J.D.F. (1985). Spectral response of a plant canopy with different soil backgrounds. *Remote Sensing of Environment*, 17, 37-53.

International Union for Conservation of Nature (IUCN). (2020). 100 of the world's worst invasive alien species. http://www.iucngisd.org/gisd/100_worst.php

Joshi, C., De Leeuw, J., van Andel, J., Skidmore, A.K., Lekhak, H.D., van Duren, I.C., & Norbu, N. (2006). Indirect remote sensing of a cryptic forest understory invasive species. *Forest Ecology and Management*, 225, 245-256.

Kim, D.-H., Sexton, J.O., Noojipady, P., Huang, C., Anand, A., Channan, S., Feng, M. & Townshend, J.R. (2014). Global Landsat-based forest-cover change from 1990 to 2000. *Remote*

Sensing of Environment, 155, 178-193.

Kokaly, R.F., Clark, R.N., Swayze, G.A., Livo, K.E., Hoefen, T.M., Pearson, N.C., Wise, R.A., Benzel, W.M., Lowers, H.A., Driscoll, R.L., & Klein, A.J. (2017). USGS Spectral Library Version 7: U.S. Geological Survey Data Series 1035, 61 p., https://doi.org/10.3133/ds1035

Liu, J., Dietz, T., Carpenter, S.R., Alberti, M., Folke, C., Moran, E., Pell, A.N., Deadman, P., Kratz, T., Lubchence, J., Ostrom, E., Ouyang, Z., Provencher, W., Redman, C.L., Schneider, S.H. & Taylor, W.W. (2007). Complexity of coupled human and natural systems. *Science*, 317, 1513-1516.

Liu, H. & Huete, A. (1995). A feedback based modification of the NDVI to minimize canopy background and atmospheric noise. *IEEE Transactions on Geoscience and Remote Sensing*, 33, 457–465.

Lishawa, S.C., Treering, D.J., Vail, L.M., McKenna, O., Grimm, E.C., & Tuchman, N.C. (2013). Reconstructing plant invasions using historical aerial imagery and pollen core analysis: *Typha* in the Laurentian Great Lakes. *Diversity and Distributions*, 19, 14-28.

Lockwood, J.L., Hoopes, M.F., & Marchetti, M.P. (2013). *Invasion Ecology*. Hoboken, NJ: Wiley-Blackwell.

Manson, S.M. (2002). Calibration, verification, and validation. In D. C. Parker, T. Berger & S. M. Manson (Eds.), *Meeting the Challenge of Complexity*, Vol. 2.4, pp. 42-47. London: UCL Press.

McCormick, C.M. (1999). Mapping exotic vegetation in the Everglades from large-scale aerial photographs. *Photogrammetric Engineering & Remote Sensing*, 65, 179-184.

Milly, P.C.D., Betancourt, J., Falkenmark, M., Hirsch, R.M., Kundzewicz, Z.W., Lettenmaier, D.P. & Stouffer, R.J. (2008). Stationarity is dead: Whither water management? *Science* 319, 573-574.

Murphy, S.T., Subedi, N., Jnawali, S.R., Lamichhane, B.R., Upadhyay, G.P., Kock, R. & Amin, R. (2013). Invaisve mikania in Chitwan National Park, Nepal: the threat to the greater one-horned rhinoceros *Rhinoceros unicornis* and factors driving the invasion. *Oryx*, 47, 361-368.

Nagendra, H. (2002). Tenure and forest conditions: community forestry in the Nepal Terai. *Environmental Conservation*, 29, 539-539.

NASA/METI/AIST/Japan Spacesystems, and U.S./Japan ASTER Science Team (2019). ASTER Global Digital Elevation Model V003 [Data set]. NASA EOSDIS Land Processes DAAC. Accessed 2019-12-30 from https://doi.org/10.5067/ASTER/ASTGTM.003

Pearce, J. & Ferrier, S. (2000). Evaluating the predictive performance of habitat models developed using logistic regression. *Ecological Modelling*, 133, 225-245.

Pearlstine, L., Portler, K.M., & Smith, S.E. (2005). Textural discrimination of an invasive plant, *Schinus terebinthifolius*, from low altitude aerial digital imagery. *Photogrammetric Engineering & Remote Sensing*, 71, 289-298.

Pejchar, L., & Mooney, H.A. (2009). Invasive species, ecosystem services and human well-being. *Trends in Ecology & Evolution*, 24, 497-504.

Peterson, E.B. (2005). Estimating cover of an invasive grass (*Bromus tectorum*) using tobit regression and phenology derived from two dates of Landsat ETM+ data. *International Journal of Remote Sensing*, 26: 2491-2507.

Phillips, S., Anderson, R., & Schapire, R. (2006). Maximum entropy modeling of species geographic distributions. *Ecological Modeling*, 190, 231-259.

Phillips, S., & Dudik, M. (2008). Modeling of species distributions with Maxent: new extensions and a comprehensive evaluation. *Ecography*, 31, 161-175.

Potapov, P., Yaroshenko, A., Turubanova, S., Dubinin, M., Laestadius, L., Thies, C., Aksenov, D., Egorov, A., Yesipova, Y., Glushkov, I., Karpachevskiy, M., Kostikova, A., Manisha, A., Tsybikova, E. & Zhuravleva, I. (2008). Mapping the world's intact forest landscapes by remote sensing. *Ecology and Society*, 13, 51.

Powell, R.L., Roberts, D.A., Dennison, P.E., & Hess, L.L. (2007). Sub-pixel mapping of urban land cover using multiple endmember spectral mixture analysis: Manaus, Brazil. *Remote Sensing of Environment*, 106, 253-267.

Qi, J., Chehbouni, A., Huete, A.R., Kerr, Y.H. & Sorooshian, S. (1994). A modified soil adjusted vegetation index. *Remote Sensing of Environment*, 48, 119.

RECOFTC (Center for People and Forest) (2013). Community forestry in Asia and the Pacific: Pathway to inclusive development. Bangkok.

Roberts, D.A., Dennison, P.E., Gardner, M.E., Hetzel, Y., Ustin, S.L. & Lee, C.T. (2003). Evaluation of the potential of Hyperion for fire danger assessment by comparison to the Airborne Visible/Infrared Imaging Spectrometer. *IEEE Transactions on Geoscience and Remote Sensing*, 41, 1297-1310.

Roberts, D.A., Dennison, P.E., Roth, K.L., Dudley, K., & Hulley, G. (2015). Relationships between dominant plant species, fractional cover and land surface temperature in a Mediterranean ecosystem. *Remote Sensing of Environment*, 167, 152-167.

Roberts, D.A., Gardner, M., Church, R., Ustin, S., Scheer, G., & Green, R. (1998). Mapping chaparral in the Santa Monica Mountains using multiple endmember spectral mixture models. *Remote Sensing of Environment*, 65, 267-279.

Roberts, D.A., Halligan, K., & Dennison, P.E. (2007). VIPER Tools user manual. Visualization and Image Processing for Environmental Research Laboratory, Department of Geography, University of California, Santa Barbara.

Roberts, D.A., Smith, M.O., & Adams, J.B. (1993). Green vegetation, nonphotosynthetic vegetation, and soils in AVIRIS data. *Remote Sensing of Environment*, 44, 255-269.

Roth, K.L., Roberts, D.A., Dennison, P.E., Alonzo, M., Peterson, S.H., & Beland, M. (2015). Differentiating plant species within and across diverse ecosystems with imaging spectroscopy. *Remote Sensing of Environment*, 167, 135-151.

Rouse, J.W., Hass, R.H., Schell, J.A. & Deering, D.W. (1973). Monitoring vegetation systems in the Great Plains with ERTS. In Proceedings of the Third ERTS Symposium, edited by S. C. Freden et al., 309-317. Washington, DC: NASA.

Saleska, S.R., Didan, K., Huete, A.R. & da Rocha, H.R. (2007). Amazon forests green-up during 2005 drought. *Science*, 318, 612

Samanta, A., Ganguly, S., Hashimoto, H., Devadiga, S., Vermote, E., Knyazikhin, Y., Nemani, R.R. & Myneni, R.B. (2010). Amazon forests did not green-up during the 2005 drought. *Geophysical Research Letters*, 37, L05401.

Shen, M., Sun, Z., Wang, S., Zhang, G., Kong, W., Chen, A. & Piao, S. (2013). No evidence of continuously advanced green-up dates in the Tibetan Plateau over the last decade. *PNAS*, 110, E2329.

Somers, B. & Asner, G.P. (2013). Multi-temporal hyperspectral mixture analysis and feature selection for invasive species mapping in rainforests. *Remote Sensing of Environment*, 136, 14-27.

Souza Jr., C.M., Roberts, D.A. & Cochrane, M.A. (2005). Combining spectral and spatial information to map canopy damage from selective logging and forest fires. *Remote Sensing of Environment*, 98, 329-343.

Souza Jr., C.M., Siqueira, J.V., Sales, M.H., Fonseca, A.V., Riberio, J.G., Numata, I., Cocharane, M.A., Barber, C.P., Roberts, D.A. & Barlow, J. (2013). Ten-year Landsat classification of deforestation and forest degradation in the Brazilian Amazon. *Remote Sensing*, 5, 5493-5513.

Spiteri, A., & Nepal, S. (2008). Distributing conservation incentives in the buffer zone of Chitwan National Park, Nepal. *Environmental Conservation*, 35: 76-86.

Taylor, S.L., Hill, R.A., & Edwards, C. (2013). Characterizing invasive non-native Rhododendron ponticum spectra signatures with spectroradiometry in the laboratory and field: Potential for remote mapping. *ISPRS Journal of Photogrammetry and Remote Sensing*, 81, 70-81.

Tiwari, S., Adhikari, B., Siwakoti, M. & Subedi, K. (2005). An inventory and assessment of invasive alien plant species of Nepal. IUCN, Kathmandu, Nepal.

Tuanmu, M., Vina, A., Bearer, S., Xu, W., Ouyang, Z., Zhang, H., & Liu, J. (2010). Mapping understory vegetation using phenological characteristics derived from remotely sensed data. *Remote Sensing of Environment*, 114, 1833-1844.

Underwood, E., Ustin, S., & DiPietro, D. (2003). Mapping nonnative plants using hyperspectral imagery. *Remote Sensing of Environment*, 86, 150-161.

United Nations (2016). The 2030 Agenda for Sustainable Development (17 Sustainable Development Goals). Retrieved from https://www.un.org/sustainabledevelopment/sustainable-development-goals/.

Wilfong, B.N., Gorchow, D.L., & Henry, M. C. (2009). Detecting an invasive shrub in deciduous forest understories using remote sensing. *Weed Science*, 57, 512-520.

Zhang, L.L., & Wen D.Z. (2009). Structural and physiological responses of two invasive weeds, *Mikania micrantha* and *Chromolaena odorata*, to contrasting light and soil water conditions. *Journal of Plant Research*, 122, 69-79.

Zhang, G., Zhang, Y., Dong, J. & Xiao, X. (2013). Green-up dates in the Tibetan Plateau have continuously advanced from 1982 to 2011. *PNAS*, 110, 4309-4314.

Zvoleff, A., & An, L. (2014). The effect of reciprocal connections between demographic decision making and land use on decadal dynamics of population and land-use change. *Ecology and Society*, 19(2), 31.

7. Appendix A: Model Documentation

The agent-based model developed in Chapter IV was built in NetLogo 6.0. The code and documents are fully accessible at https://www.comses.net/codebases/da200968-4feb-4e17-8662-b56d026b894b/releases/1.0.0/.

8. Appendix B: ODD Protocol

The ODD (Overview, Design concepts, & Details) Protocol is adopted to document the purpose, framework, variables, and data of the agent-based model developed in Chapter IV (Grimm et al., 2006; Grimm et al., 2010).

1. Purpose

This model serves three purposes:

1) To model local households' participation in intervention of invasive *M. micrantha* in the western Chitwan community forests. Household's decision in participation will be determined by a suite of socioeconomic, demographic and geographic characters.

2) To simulate the responses of *M. micrantha*'s extent to the intervention.

3) To produce real-world projections of *M. micrantha* invasion based on household attributes and intervention practices.

2. Entities, state variables, and scales

One time-step represents one year and simulations will run for 25 years. One grid cell represents an area of 30m by 30m, and the model landscape comprises 1083 by 614 cells.

Entities of the model include Household (social module) and the Environment cells (ecological module):

1) Household agents have geographic attributes (distance to community forests) and socioeconomic attributes (household size, use firewood or nor, participate in user groups or not). The household agents have state variable of participating in *M. micrantha* intervention or not. One pixel represents one non-moving household. In every step, household's socioeconomic attributes will be changed. These changes are informed by the changing trend

between two waves of household survey conducted in 2014 and 2017, respectively. In every step, there is a chance that the household will participate in the intervention. This chance is based on a regression equation that includes the above geographic and socioeconomic attributes.

2) Environment (grid cell) has attributes of being invaded or not. One environmental grid cell represents a 30 m by 30 m, or 900 m^2 area. In every time step, if the environment is not invaded, and if one of its neighbors is invaded in the last time step, it may be invaded based on the probabilities determined by the parameter "Invasion rate". In terms of intervention, starting in Time 5, *M. micrantha* in certain amount of forests cells will be cleaned based on the simulated participating households. Selection of the cells will be based on their distances to the households and closer cells have higher priority being selected.

3. Process overview and scheduling

Possible agent actions are as follows:

1) Model (Step 0 only, Year 2015): Create and set up household agents and environmental grids

2) Household (each step, social module): attributes change (starting in Time 3, year 2018) and participate in intervention (starting in Time 5, Year 2020)

3) Environment (each step, ecological module only): *M. micrantha* spread to neighboring landscape cells, and being cleaned by intervention (starting in Time 5, Year 2020)

4. Design concepts

4.1 Basic principles

Social module – This module assumes that household's participation in *M. micrantha* intervention is affected by a suite of geographic and socioeconomic attributes. This relationship is informed by the household survey conducted in 2017, and household's probability in

participation is quantified through a logistic regression. The cost of time and labor in cleaning certain area of forest landscape is quantified through field experiments conducted between 2015 and 2018 (Clark 2020).

Ecological module – It is a cellular automaton-based model to simulate the spread of *M. micrantha* in the forests. In every time step, if the environment is not invaded, it will be invaded if one of its neighbors is invaded in the last time step, based on a probability determined by the parameter "Invasion rate".

4.2 Emergence

Social module: The change of household's socioeconomic attributes may have more or less of an impact than expected.

Ecological module: The invasion rate (probabilities of *M. micrantha* spreading from current invaded cells to neighboring cells) may have more or less an impact than expected.

4.3 Adaptation

Social module: Household agents decide on their intervention participation based on their geographic and socioeconomic attributes.

4.4 Objectives

Social module: Household agents' only objective is to remove *M. micrantha* from the forests.

4.5 Learning

In this model, agents do not change their adaptive traits over time as a response of their experience.

4.6 Prediction

Agent's decisions are made based on information available at the current step, instead of

considering possible future outcomes.

4.7 Sensing

Not sensing is identified in this model.

4.8 Interaction

No interactions are identified in this model.

4.9 Stochasticity

Social module: Household socioeconomic attribute changes are informed by the differences between two waves of household surveys and they are partially stochastic. Household intervention participation is based on a probability quantified through household attributes, so their decision in participation is partially stochastic.

Ecological module: The probability of *M. micrantha* spread to neighboring cells is partially stochastic.

4.10 Collectives

No collectives are identified in this model.

4.11 Observation

The outputs of the model include two .csv files: One depicting the number of household participating in intervention in every step, and one plotting the percentage of forest non-water cells being invaded in every step. Other outputs include the spatial distribution maps of the invaded cells.

5. Initialization

All initial values of household attributes are informed by the 2017 household survey. Initial *M. micrantha* extent in the forests are adopted from Dai et al. (2020).

6. Input data

Household attributes are derived from the household survey conducted in 2017. Their changes follow the trends informed by the differences between the 2014 and 2017 surveys. The cost of labor and time in intervention are examined by Clark (2020). Initial *M. micrantha* extent in the forests are adopted from Dai et al. (2020).

7. Submodels

The processes for the two submodels are summarized below.

1) Step 0: All agents and environment types (households and the environment) are created and parametrized.
2) Social module: Household geographic attribute (distance to community forest) is constant throughout the modeling process, whereas the socioeconomic and demographic attributes will vary according to the differences between 2014 and 2017 household surveys. In every step, the new livestock amount was set to be its previous value minus a Poisson-distributed random integer with a mean of 1.011/3. If the new value was negative, we also set it to be zero. The probability of a household switching from using firewood to not using is 0.0744/3, and the probability of switching from not using to using is 0.5604/3. If a household participated in a user group last, the probability of not participating this time is 0.2513/3. If a household did not participate in any user groups last time, the probability of participate in at least one this time is 0.8225/3. If the household held community forest membership last time, the probability of not holding any more is 0.1722/3. The probability of switching from not holding to holding is 0.3213/3. If the household farmed last time, the probability of not farming this time is 0.0922/3. The probability of the opposite direction of change is

0.3005/3. If the household had business incomes last time, the probability of not having anymore this time is 0.3115/3. The probability of the opposite direction of change is 0.1613. If a household had income from salary jobs last time, the probability of not keeping it is 0.3166/3. The probability of the opposite direction of change is 0.2483/3. Given the geographic and socioeconomic attributes, the household's probability of intervention participation is calculated based on Equation 1. In the modeling process, if a randomly generated number between 0 and 1 is smaller than this probability, the corresponding household will contribute labor to *M. micrantha* intervention in the current step.

3) Ecological module: In this cellular automata-based module, for a target cell, if it is not invaded this time and any of its neighbors are invaded, the probability of it being invaded is based on a model input (0.2, 0.5, 0.8 or 1.0). Once *M. micrantha* is removed, the corresponding cell will not be marked as invaded afterwards, unless it is re-invaded in later steps.